

Advanced Deep Learning Approaches in Metasurface Modeling and Design: A Review

Yunxi Dong¹, Sensong An^{2*}, Haoyue Jiang², Bowen Zheng¹, Hong Tang¹, Yi Huang¹, Huan Zhao¹,
Hualiang Zhang^{1*}

¹*Department of Electrical & Computer Engineering, University of Massachusetts Lowell, Lowell, Massachusetts 01854, USA*

²*Department of Electrical Engineering, University of North Texas, Denton, Texas, 76205, USA*

[*Sensong.An@unt.edu](mailto:Sensong.An@unt.edu), Hualiang.Zhang@uml.edu

Abstract

Nanophotonic devices have marked a significant advance in light control at the subwavelength level, achieving high efficiency and multifunctionality. However, the precision and functionality of these devices come with the complexity of identifying suitable meta-atom structures for specific requirements. Traditionally, designing metasurface devices has relied on time-consuming trial-and-error methods to match target electromagnetic (EM) responses, navigating an extensive array of possible structures. Recently, deep learning(DL) has emerged as a potent alternative, streamlining the forward modeling and inverse design process of nanophotonic devices. This review highlights recent strides in deep-learning-based photonic modeling and design, focusing on the fundamentals of various algorithms and their specific applications, and discusses the emerging research opportunities and challenges in this field.

Key Words

Metasurface, Nanophotonic, Deep learning, Artificial intelligence, Inverse design

Highlights

- Exploration of how DL techniques streamline metasurface design, offering a leap in efficiency compared to traditional methods.
- In-depth analysis of various DL models, including autoencoders (AEs), tandem neural networks (TNNs), and generative adversarial networks (GANs), in the context of metasurface design and modeling.
- Identification of specific areas in metasurface design where artificial intelligence (AI) can make a significant impact.
- Future directions for integrating AI in metasurface technology, underlining areas that need further research and development.
- Challenges and real-world applications.

1. Introduction

Metasurfaces, essentially two-dimensional arrays of artificial structures, have garnered significant attention for their ability to manipulate EM waves with precision and flexibility [1,2]. Metasurfaces are ultra-thin, engineered structures that have the ability to manipulate EM waves in ways that traditional materials cannot. They are composed of meta-atoms, which are the individual, sub-wavelength building blocks tailored to impose specific local alterations to the EM field. The materials used in creating metasurfaces can vary widely, ranging from metals [3] to dielectric

compounds, such as silicon [4] and titanium dioxide [5], which are chosen based on their interaction properties with specific wavelengths of EM waves. These ultrathin layers of nanostructures enable unprecedented control over light's properties, including phase, amplitude, polarization, and direction. The ability to tailor these aspects opens up a plethora of applications in areas such as advanced optics, telecommunications, sensing, and even quantum computing.

Designing and modeling these complex structures, however, presents a formidable challenge. Traditional approaches often involve iterative and computationally intensive numerical simulations to explore the vast design space and achieve the desired optical responses [6–10]. This process is not only time-consuming but also requires a deep understanding of EM theory and material science. The advent of DL offers a paradigm shift in this field. Deep neural networks (DNNs) [11,12], inspired by the structure of biological neural networks, function as intricate models characterized by numerous adjustable parameters. These networks are trained using extensive datasets that map inputs to outputs, allowing the fine-tuning of their parameters for precise predictions on new data. DNNs boast a significant number of adjustable elements, often exceeding millions of parameters. This vast array of choices, along with the diverse range of neural network architectures that are available, makes them exceptionally efficient for accurately predicting complex input-output relationships in various systems [13–16]. Notably, DNNs have proven to be remarkably effective in correlating the physical attributes of nanostructures with their EM behaviors [17–20]. Leveraging powerful computational models, it is now possible to predict the optical responses of metasurface more efficiently, optimize their design, and even discover new configurations that were previously unattainable through conventional methods [18,21]. The integration of DL into metasurface design and modeling represents a cutting-edge blend of photonics and artificial intelligence, heralding a new era of rapid, efficient, and innovative development in nanophotonics.

This review paper explores the transformative intersection between advanced computational methods and nanophotonic engineering, focusing on the use of DL in the design and modeling of metasurfaces. It covers two main categories: forward modeling and inverse design, each employing various types of DNNs such as fully connected neural networks (FCNNs) [22,23], convolutional neural networks (CNNs) [23–26], tandem neural networks (TNNs) [27], autoencoders (AEs) [28], and generative adversarial networks (GANs) [29–31]. These networks are foundational tools that offer unique capabilities to address the complex challenges of metasurface design.

Forward-predicting networks, discussed in Section 2 of the paper, are designed to learn the relationship between the structural parameters of metasurfaces and their EM responses, serving as rapid, low-cost alternatives to full-wave simulators. Inverse design networks, introduced in Section 3, leverage neural networks to find the optimal metasurface structures for achieving desired EM responses, incorporating forward-predicting models like TNNs or GANs to validate design predictions during training.

This review is structured to first introduce forward-predicting networks followed by inverse design networks, providing a comprehensive overview of how these technologies enable rapid advancements in metasurface technology through the integration of AI. This structured approach helps to illustrate the potential applications, strengths, and limitations of these DL techniques in a coherent and practical framework. To provide readers with a comprehensive understanding of recent advancements in this area, we include Table 1. This table outlines the DL techniques, the specific DNN input and output parameters, and the design geometries of meta-atoms used in notable recent studies. Examples in the table range from metasurface beam deflectors to optical filters and metalenses, illustrating the versatility and broad application spectrum of these DL techniques.

DL Algorithm	Network Input	Network Output	Design geometry	Working Bandwidth	Application
AE [32]	Structured-light image (RGB)	Depth map (1 channel)	Cuboid and hexagonal column	Visible light spectrum	Lens
AE [33]	Transmission spectrum	Classification results	Quasi-free-form	300 - 850 nm and 1550 -1650 nm	User-defined modulator
AE [34]	Geometric parameters of a super meta-atom	Geometric parameters	Cuboid	1550 nm	Lens
AE [35]	Far-field radar cross section (RCS)	Metasurface combinations and arrangements	Cylinder	8, 8.1, 8.2 GHz	Intelligent surface for satellite communication
Conditional VAE [36]	Reflection coefficient at 40 - 60 THz	Reflection coefficient of 60 - 100 THz	Cylinder and elliptical cylinder	40 - 60 THz	User-defined modulator
Residual AE [37]	Electric field distribution (28*28)	Handwritten number images	Free-form	Visible	Hologram
Adversarial AE [38]	Meta-atom shapes, design parameters, predefined model distribution	2D patterns	Free-form	0.5 - 1.75 μ m	Thermal Emitters
AE [39]	Reflection spectrum and latent variable	2D patterns	Free-form	40 - 100 THz	User-defined modulator
FCNN [40]	13-layer thickness	Reflection spectrum	Stack of thin films	177 - 210 THz	Multilayer metamaterial for computing applications
FCNN [41]	Mie coefficients of a meta-atom	Mie angles	Sphere	800-1200 nm	User-defined modulator
FCNN [42]	Layer thickness	Transmission spectrum	Stack of thin films	400 - 700 nm	User-defined modulator
FCNN [43]	Membrane radius, thickness, cavity depth, and frequency	Absorption spectrum	Cylinder	0 - 300 THz	Acoustic absorber
FCNN [17]	Geometric parameters	Transmission spectrum	Cylinder, H-shape	30 - 60 THz	User-defined modulator
FCNN [44]	Geometric parameters	Transmission spectrum	Cylinder	4 - 5 μ m	Lens
FCNN [45]	Geometric parameters	Reflection spectrum	Cylinder	400 - 700 nm	Color generation

FCNN [46]	Geometric parameters	Transmission phase and amplitude	Cylinder	940 nm	Lens
FCNN [47]	Geometric parameters	Reflection spectrum	Cylinder	380 - 780 nm	Sensor
FCNN [48]	Thickness of nanoparticle shells	Scattering cross section	Sphere	400 - 800 nm	User-defined modulator
TNN [49]	Reflection spectrum	Geometric parameters	Cube	1 - 41 GHz	Microwave absorbers
TNN [50]	Far-field and near-field spectrum	Meta-atom arrangement patterns	Cylinder	8 - 11 GHz	Metasurface cloak
TNN [51]	Reflection spectrum	5-dimensional design vectors	Ring	1 - 10 GHz	Reflection reduction metasurface
TNN [27]	Transmission spectrum	Layer thickness	Stack of thin films	400 - 1000 nm	User-defined modulator
TNN [52]	Spectrum (reflection and absorption)	Geometric parameters	1D grating	500 - 700 nm	User-defined modulator
TNN [53]	Transmission spectrum	Geometric parameters	1D grating	1300nm - 1600 nm	Grating coupler
TNN [45]	Reflection spectrum (converted to color values)	Geometric parameters	Cylinder	400 - 700 nm	Color generation
CNN [54]	Metamaterial structures and spectral data	Similarity of this pair to other potential designs and their spectrum	Concentric rings	2 to 30 GHz	User-defined modulator
CNN [55]	1-D structures	Coupling efficiency	Cuboid	1550 nm	Grating coupler
CNN [56]	Meta-atom patterns	Transmission spectrum	Quasi-free-form	640 - 780 nm	Optical collimator
CNN [57]	Meta-atom patterns	Reflection spectrum	Free-form	600 - 100 nm	Polarization-control metasurface
CNN [58]	Meta-atom patterns	Transmission phase and amplitude	Free-form	30 - 60 THz	Lens
CNN [18]	Meta-atom and neighbor patterns	Transmission phase and amplitude	Free-form	5.45 μ m	Beam deflector and lens
CNN [59]	Meta-atom patterns	Absorption spectrum	Free-form	800 - 1700 nm	User-defined modulator
CNN [20]	3-D nanostructure models	Electric polarization	Free-form	700 nm	User-defined modulator
GAN [60]	Latent space	Meta-atom patterns	3-layers free-form	8 - 12 GHz	User-defined modulator

Conditional GAN [61]	Latent vector and design targets	Geometric parameters	Stack of thin films	Visible	Structural color filter
Conditional DCGAN [62]	Noise and input spectrum	2D patterns	Free-form	250 - 500 THz	User-defined modulator
Conditional GAN [63]	Desired wavelength and deflection angles	2D patterns	Free-form	600 - 1300 nm	Beam deflector
Conditional GAN [64]	Latent space and transmittance	2D patterns	Free-form	170 - 600 THz	User-defined modulator
Conditional GAN [65]	Noise and contrast vector	2D patterns	Free-form	400 - 680 nm	User-defined modulator
Conditional WGAN [21]	Latent vector and target phase and transmittance	2D patterns	Free-form	6 μ m	Multifunctional beam deflector, lens

Table 1. Overview of recent works on DL implementation on metasurface modeling and design. Columns from left to right: DL techniques, DNN input and output parameters, design geometry of meta-atoms, working bandwidth for metasurface device and device function.

2. Forward-Predicting Networks

The objective of a forward neural network is to process the physical attributes of a nanophotonic structure, such as its geometry and materials, to predict its EM response. In doing so, it emulates the functionality of full wave simulators but with significantly faster computation times (usually in milliseconds timescale). This makes it highly suitable for integration with optimization algorithms or DNNs for inverse design purposes. With adequate training data, these networks are capable of accurately characterizing the EM responses of metasurfaces. In previous studies, various types of DNN architecture have been explored for the purpose of forward prediction. For example, FCNNs [17,40–48,66–78] are particularly favored for simpler structures due to their simplicity and versatility. For more complex structures, the effectiveness of 2D convolutional networks becomes pronounced as they process these structures as images [18,58,59], greatly aiding in the accuracy of predictions while requiring less computational resources such as memory. Lastly, sequential neural networks like recurrent neural networks (RNNs) [79,80] and 1D convolutional networks [81] are optimal for EM spectra predictions, given their sequential nature and the high correlation between adjacent spectral points. In the following sections, we introduce the various forward-predicting networks, along with representative works for each category.

2.1 Fully Connected Neural Networks (FCNNs)

FCNNs, often termed as a dense network, represents a powerful class of artificial neural networks that are characterized by the connectivity of each neuron in one layer to every neuron in the subsequent layer [22,23]. These networks are one of the most straightforward and widely used architectures in the realm of DL. They consist of multiple layers of nodes, including an input layer, several hidden layers, and an output layer, with each layer fully connected to the next. The strength of fully connected networks lies in their versatility and capacity to model complex, non-linear relationships by adjusting weights and biases through learning algorithms, typically backpropagation. However, the architecture's requirement for a high number of parameters often makes it computationally intensive and prone to overfitting [11,12,23,82], especially in scenarios with limited data or highly

dimensional input spaces such as transmission spectrum . Despite these challenges, FCNNs continue to be a foundational building block and a starting point for understanding deeper architectures and concepts in neural networks. In recent years, the implementation of FCNNs in aiding metasurface design has emerged as a transformative approach. This approach first signifies a shift from the traditional, time-consuming trial and error methodologies [1,2] to more efficient and accurate design processes enabled by DL techniques. FCNNs, with their dense and intricate architectures, have proven to be particularly adept at capturing the complex interactions and dependencies characteristic of metasurface structures[17,40–44,46–48,66–78].

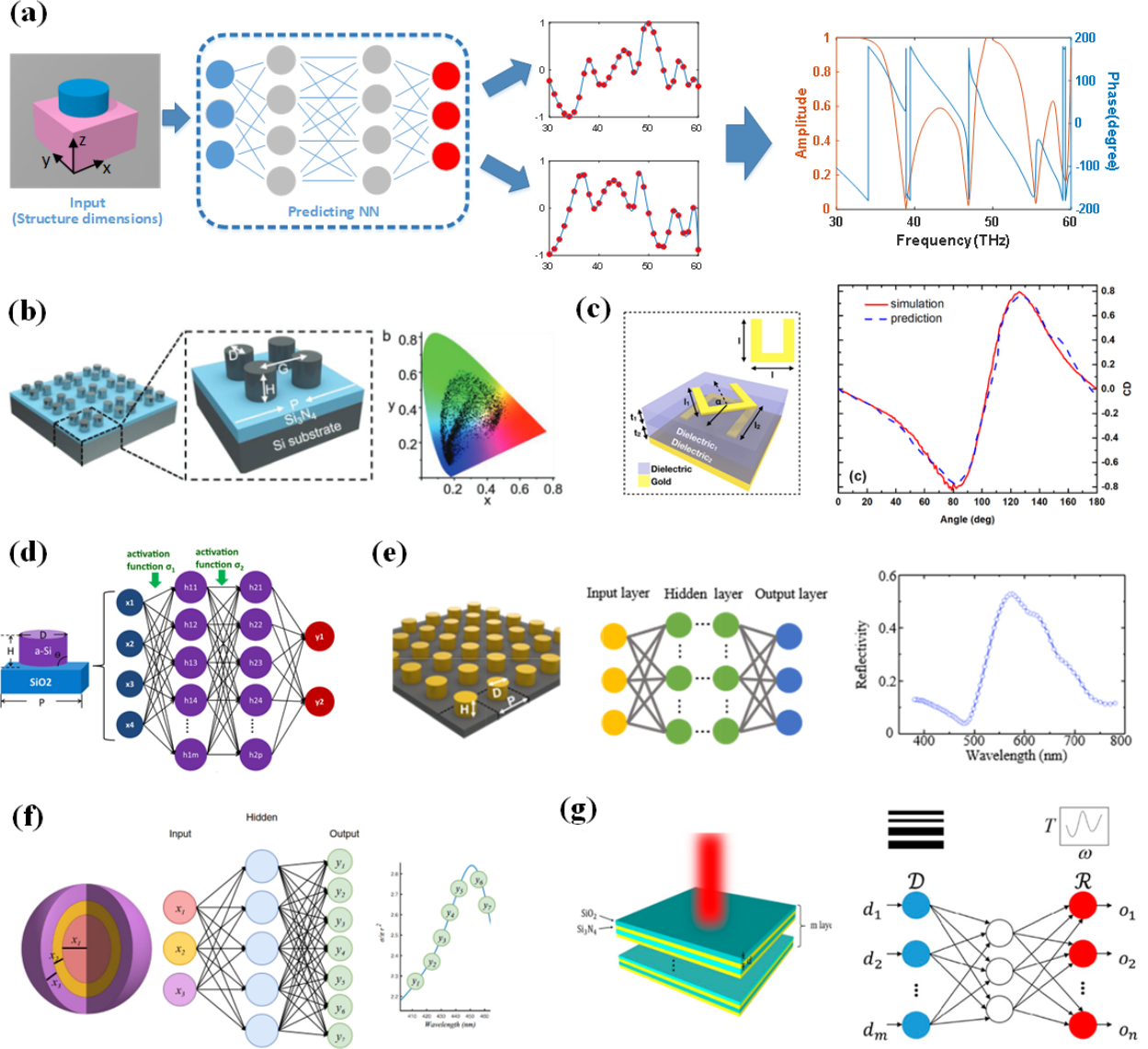


Figure 1. FCNNs in optical metasurfaces and photonics. **a**, a standard forward prediction flow from ref. [17]. The network will pass the meta-atom's structure dimension as input to predicting model to output EM response at specific frequencies **b**, a forward predicting network that predicts the color information of Silicon meta-atoms based on their dimensions in ref. [45] **c**, an FCNN in ref. [83] that predicts the reflection spectra based on the design parameters of chiral metasurface. **d**, an FCNN in ref. [46] that predicts the phase and transmission of cylindrical Si-on-SiO₂ meta-atoms. **e**, an FCNN in ref. [47] to predict the reflectivity of cylinder meta-atoms. **f**, an FCNN in ref. [48] with the thickness of each shell of a nanoparticle as input and its scattering cross section at different

wavelengths as output. **g**, a forward predicting network in ref. [27] with the thicknesses of SiO_2 and Si_3N_4 thin films as input and the transmission spectra as output.

In prior studies involving FCNNs for metasurface analysis and characterizations, the networks typically process the design parameters of the meta-atoms. They use these parameters as input to generate the corresponding spectrum, which include factors such as transmission, reflection, and the phase and amplitude responses of meta-atoms. In the paper by An et al. [17], an FCNN approach for forward prediction in the characterization of metasurface (Fig. 1a) is introduced. This network focuses on accurately predicting the EM responses of cylindrical meta-atoms based on their design parameters. In this work, the authors use real and imaginary parts of transmission coefficients as outputs of the FCNN, effectively reducing the prediction errors associated with resonances and phase discontinuities. The paper by Gao et al. [45] focuses on a forward prediction network for accurately determining the color outcomes of silicon nanostructures (Fig. 1b). This network uses the geometric parameters of the nanostructures as inputs and predicts their color characteristics. The network is trained with a large dataset to ensure precise predictions, making it a valuable tool in the design and optimization of structural color applications in nanophotonics.

The paper by Ma et al. [83] introduces an FCNN model for forward prediction in the design of chiral metamaterials (Fig. 1c). This model uses a DNN to map geometric parameters of metamaterials to their optical responses. The emphasis is on accurately predicting the full optical responses of chiral structures under various polarization conditions. The paper by Lin et al. [46] discusses an FCNN model for forward prediction in the design of high numerical aperture near-infrared metalenses (Fig. 1d). The DNN model is used to optimize the metalens design by predicting its optical performance based on input design parameters.

The study by Li et al. [47] presents an FCNN for modeling plasmonic sensors (Fig. 1e). This forward prediction network efficiently uses the geometric parameters of nanostructures to predict their optical spectra. With a training dataset comprising two thousand simulations, the FCNN can quickly and accurately predict spectra for a wide range of nanostructures. This method significantly reduces the need for extensive simulations, enhancing the design process of plasmonic sensors. The network's predictions maintain a high accuracy level, with over 97.5% of them having less than 5% error.

Other than predicting using geometric parameters, FCNNs can also be used to predict the EM response of multilayer structures. The paper by Peurifoy et al. [48] discusses a forward prediction network based on FCNN architecture for nanophotonic particle simulation and inverse design (Fig. 1f). This network efficiently processes input parameters of nanophotonic structures and predicts their optical responses. In another study, Liu et al. [27] focuses on a forward prediction network based on a FCNN framework for the inverse design of nanophotonic structures (Fig. 1g). This forward modeling network is trained to predict the optical properties of multi-layer nanophotonic designs based on their structural parameters.

These applications of FCNN significantly accelerate the design and optimization process in nanophotonics, showcasing the model's ability to learn and generalize the intricate relationship between a nanostructure's geometry and its optical characteristics, marking a substantial advancement in the field of nanophotonic design. In recent years, FCNNs have also been used in predicting the responses of multi-layer metasurface devices and metamaterials [40–42,71]. The simple structure and ease of use of FCNNs not only accelerate the design process but also open up new possibilities for optimizing and creating innovative metasurface structures that were previously unfeasible or too complex to achieve through conventional means.

2.2 Convolutional Neural Networks (CNNs)

CNNs are a specialized kind of DNNs that are highly effective for analyzing and interpreting various types of data beyond just visuals. At their core, CNNs learn to recognize patterns and features in any form of array data. The CNN we are referring to here is 2D CNNs, which deals with 2D input, different from the 1D CNNs that we will discuss in the following section. The CNNs are structured in layers, with each layer transforming the input data to allow the network to progressively understand complex structures. The convolutional layers, the most important part of CNNs, apply filters to their inputs to detect specific features such as edges or shapes in images, or patterns in other types of data like time series. Subsequently, pooling layers are introduced, which reduce the dimensionality of the data, therefore helping in reducing computation and controlling overfitting. While widely known for their application in computer vision [24–26,84], CNNs' ability to learn spatial hierarchies of features makes them suitable for a variety of tasks beyond image processing. The adaptability and success of CNNs in diverse fields stem from their architecture, which efficiently captures and learns patterns from complex, high-dimensional data [25]. The suitability of CNNs for metasurface modeling and design lies in their inherent ability to recognize and analyze spatial hierarchies and patterns within complex datasets, making CNNs a good tool to carry out metasurface design and modeling [18,19,54–59,66,73,81,85–91]. Compared to FCNNs, CNNs demonstrate a significant advantage in handling structured grid data like meta-atom images. They reduce the number of parameters through convolutional layers' local connectivity and weight sharing, making them less prone to overfitting and more computationally efficient [23,82]. In real applications, CNNs are often followed by dense layers because while CNNs excel at extracting local, hierarchical features from data (like images), dense layers are crucial for combining these features and making global, high-level decisions, such as classifying the extracted features. This synergy allows for more effective and accurate processing and interpretation of complex data, which is why they are used together instead of relying solely on CNNs, as demonstrated in the examples in Figure 2.

On recent advancements within the field, more sophisticated CNNs architectures [26,92–94] such as ResNet [55,59,87,88], neural tensor network (NTN) [58], attention module [55,87] and transfer learning [95] have been introduced to enhance the prediction of spectrum of meta-devices based on their design geometry. These evolved structures offer significant improvements over plain CNNs, as they incorporate deeper, more complex layers and learning strategies that capture an extensive range of data patterns and relationships.

In the paper by An. et al. [58], the NTN was applied to capture 1D properties features from all-dielectric free-form meta-atoms, in conjunction with a traditional CNN that processes 2D images of all-dielectric free-form meta-atoms (Fig. 2a). The utilization of CNN in this context serves the purpose of efficiently processing and analyzing the complex imagery data associated with these meta-atoms. The extracted features are then flattened and passed through two fully connected (dense) layers. This step is crucial because it integrates the extracted features into a form that can be used to uncover the hidden relationships between the meta-atom designs and their spectrum. By doing so, the DNN model is able to accurately predict the transmission spectra of given meta-atom designs, facilitating the evaluation of their performance. This approach highlights the combined strength of CNN for feature extraction and dense layers for high-level pattern recognition and prediction in complex metasurface characterizations.

In 2023, Zeng et al. employed a DL model with ResNet architecture [55], integrated with multi-head attention (MHA), to address the challenge of data shift in predicting the EM response of nano-structured metamaterials. The ResNet framework, modified for 1D input, serves as the base for extracting features from the data, while the multi-head attention mechanism enhances the model's ability to process global information. This innovative combination, referred to as ResNet-MHA, shows improved performance in dealing with data shifts compared to traditional methods, offering a significant advancement in the design and analysis of complex metasurfaces devices.

In previous works, CNNs have also been used to analyze the effects of neighboring meta-atoms, or realistic boundary conditions on metasurfaces. These studies recognize that each meta-atom within an actual metasurface is surrounded by non-identical meta-atoms, which affects near-field coupling differently from that in idealized models.

In [18], a DNN approach is introduced to better predict the EM responses of meta-atoms without assuming periodic boundary conditions (Fig. 2c). This method involves training the DNN with a large dataset, consisting of over 200,000 groups of meta-atoms with various neighbors, to predict the local response of a meta-atom based on its dimensions and neighbors. The trained CNN then uses this information to accurately predict local responses, facilitating the optimization of metasurfaces impacted by mutual coupling. This approach has successfully improved the focusing efficiency of high numerical aperture metalens by over 20%.

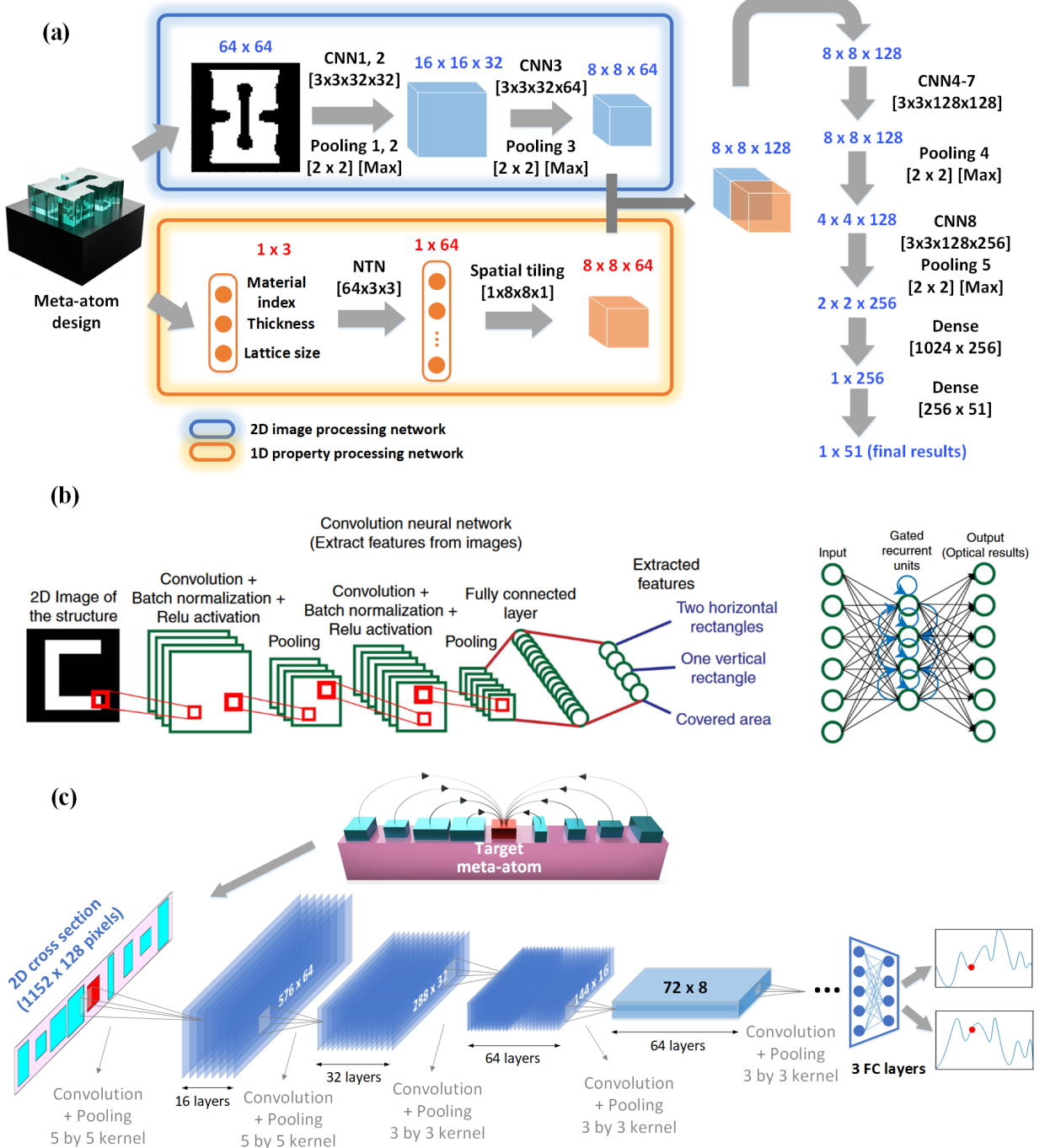


Figure 2. CNN in optical metasurfaces and photonics. **a**, a CNN in ref. [58] to predict the transmission spectrum of free form all-dielectric meta-atoms, with the cross-sections of the meta-atoms as the input and the transmission

spectra as the output. **b**, a CNN in ref. [59] that predicts the absorption spectra of meta-atoms based on their 2D cross sections. **c**, a CNN in ref. [18] that predicts the realistic performance of the center target meta-atom given the shape and dimensions of all its neighbors.

2.3 Sequential Neural Networks

Determining the EM response of a metasurface across a frequency range is crucial, even in monochromatic applications where evaluating a narrow bandwidth near the target frequency is key to assessing design robustness. Viewing the EM response as a correlated sequence rather than isolated data points offers significant informational advantages. Therefore, a DNN designed to evaluate sequences inherently outperforms one that analyzes individual data points, due to the strong correlations between adjacent points in the spectrum.

There are two primary types of sequential neural networks utilized for predicting metasurfaces' EM responses, namely recurrent neural networks (RNNs) [96] and 1-dimensional convolutional neural networks (1D CNN) [97]. RNNs are functioning by merging the feedback from their output sequences with incoming inputs to anticipate future points in the sequence, while the 1D CNN operates by detecting common sequential patterns, termed filters, within the dataset. These networks learn the most effective filters and their associated weights from the training data, enabling them to make precise sequence predictions. Both kinds of networks have the capacity to develop comprehensive forward-predicting networks. Such networks can be trained to determine the EM responses of a wide range of structures and materials across various segments of the EM spectrum, and both will be detailed in the following sections.

2.3.1 Recurrent Neural Networks (RNNs)

RNNs are primarily employed for predicting sequential data, excelling in narrowband applications. Unlike traditional DNNs, which process inputs independently, RNNs have loops allowing information to persist. This looping mechanism makes them ideal for tasks where context and order in a sequence are important. However, RNNs face challenges with long sequences, leading to a preference for long short-term memory (LSTM) [98,99] or gated recurrent unit (GRU) [100] layers over the simpler RNN layer. LSTM and GRU can handle sequences up to around 100 data points by detecting both long-range and short-range patterns. While LSTM may offer slightly better accuracy, GRU cells are less complex, enabling faster training and computation [96,99,100].

In practice, one might start with GRU for initial network architecture experiments and later switch to LSTM for the final design. RNNs, similar to fully connected layers, can have LSTM or GRU layers stacked, but generally with fewer neurons per layer due to computational intensity. It's crucial to set each layer to "return sequences" for processing the full sequence, not just the final point. Unique to EM spectra prediction, a branching network approach can be utilized, starting sequences at both the highest and lowest frequencies, then averaging the predictions [79,80]. This technique compensates for the difficulty in predicting long sequences. While RNNs can be solely composed of recurrent layers, including fully connected layers after flattening the output of the last recurrent layer can enhance long-range prediction accuracy.

RNNs are not only used independently for predictions but can also be effectively combined with other DL models. This hybrid approach can enhance their predictive capabilities and applicability. In the paper by Sajedian et al. [59], the authors present a novel method for determining the optical properties of plasmonic structures (Fig. 2b). The approach combines CNNs and RNNs to process images of these structures. The primary purpose of CNN in this research is to collect spatial information from images of the structures. This spatial data is then utilized by the RNN to predict the relationship between the structure's spatial characteristics and its absorption spectrum. This method

aims to provide an efficient and accurate alternative to traditional, time-consuming numerical simulations, enabling rapid predictions of optical properties without the need for extensive computational resources.

2.3.2 1-Dimensional Convolutional Neural Networks (1D-CNNs)

As CNNs widely recognized for their success in 2D image processing, they also have a 1D variant effective for handling sequences like EM spectra [81,85,101]. These networks identify common subsequences (filters) within the data, using weighted aggregations for spectrum predictions. An advantage of 1D-convolutional networks over RNNs is their ability to directly specify filter lengths (kernels), enhancing their efficacy in predicting long sequences. Additionally, they are generally less computationally demanding and thus quicker to train than recurrent networks.

Unlike 2D image processing, where convolutional networks compress the image's natural plane, 1D-CNNs for EM spectra prediction maintain the sequence's length and shape, simplifying network assembly. This approach eliminates concerns about matching dimensions between layers and reduces hyperparameter tuning, as the stride is consistently set to one and “same” padding is used. In constructing the network, designers decide on the kernel size and the number of filters for each layer. The kernel size dictates the pattern length detected in each sequence, while the number of filters represents the variety of patterns applied to the input. Higher values for these parameters increase the network's fitting capability (and potential for overfitting), but require more computing power and training time. Optimally, the kernel size should decrease in deeper layers, while the number of filters in the final layer should match the number of output spectra.

It is crucial to clarify that 1D-CNNs are fundamentally convolutional architectures, designed to efficiently extract local feature patterns from sequential or time-series data without inherent sequential memory capabilities. This contrasts with traditional sequential neural networks, such as RNNs and LSTMs, which are built specifically to handle sequences by maintaining a memory of previous inputs in their internal state across the sequence.

As an example, the paper by Lin et al. [81] introduces an efficient network architecture utilizing 1D-CNN for the inverse design of plasmonic metasurfaces. Unlike other works which mainly use CNN to extract features from 2D cross sections of nanophotonic structures, this network is optimized for handling spectral data, efficiently identifying key features in target spectra to aid in the design process. The developed 1D-CNN network takes target absorption spectra as input and generates geometric parameters of a 3-cylinder metasurface unit cell as the output. The architecture includes several convolutional layers, each followed by a rectified linear unit (ReLU), a max-pooling layer, and batch normalization. The design emphasizes sparsity in connections and optimal parameter tuning to improve training efficiency and generalization capabilities.

3. Inverse Design Networks

The inverse design process of metasurfaces with DNNs involves inputting a desired EM response and using the DNNs to identify corresponding structures capable of producing such a response. This process performs calculation on a one-time basis, thereby eliminating the need for further optimization. However, it's more complex than forward-predicting neural networks due to two reasons: First, there may not be any structures within the neural network's domain that can achieve the desired response, requiring a method to find the closest possible structure. Second, multiple structures might produce the same response, complicating network training and often resulting in the identification of only one solution, which may not be ideal due to fabrication limitations. Three DNN architectures are deemed suitable for metasurface inverse design problems and are utilized to address these two

challenges. The TNNs, mainly based on FCNNs, typically generate one structure per response. The AEs model, comprising an encoder and a decoder, compresses input data into a smaller format and then reconstructs it. Lastly, GANs are used to produce multiple structures for similar responses. GANs involve a generator for creating structures and a discriminator for evaluating them. These networks improve via competitive training, though achieving convergence can be complex.

3.1 Tandem neural networks (TNNs)

TNNs are a sophisticated configuration in DNN architectures where two or more DNNs are connected in sequence, with each network designed to perform a specific task. This sequential arrangement allows for complex, multi-stage processing of data, where the output of one network becomes the input for the next. By incorporating a pre-trained forward model, TNNs address the challenge of non-uniqueness in inverse design by enabling the generation of multiple distinct nanostructure designs that produce similar spectrum. This approach allows for flexibility in selecting designs that meet fabrication constraints or other practical requirements while achieving the desired response.

In 2018, Liu et al. introduced TNN for designing multi-layer photonic structures [27]. This model comprises two interconnected FCNNs, one dedicated to forward prediction and the other to inverse design. Initially, the forward model is pre-trained and its weights are fixed. During the sequential training, the focus shifts to refining the inverse network by adjusting its weights to minimize the cost. The trained forward-modeling network is then connected to the inverse-design network, forming the TNN. Inputs of spectra are processed through this tandem setup, where an intermediate design output is generated and then fed into the forward model to produce the corresponding spectrum. This methodology offers a novel approach in DNN-based optimization and design of photonic structures.

Meta-filters or frequency-selective surfaces (FSS) are widely used in EM and can serve as an ideal application to showcase the TNNs' effectiveness for inverse design. The goal in designing meta-filters is to achieve a specific transmission spectrum, well-suited for tandem network implementation. The example in Fig. 3a [17] uses cylindrical dielectric meta-atoms, chosen for their simplicity and ease of fabrication. The design process involves varying the meta-atoms' physical properties, such as permittivity, size, and spacing, operating at an infrared spectrum between 30 and 60 THz. The inverse design network inputs target spectra and outputs design parameters, which are then evaluated by a forward-predicting network for their EM responses. The training process optimizes the inverse network to closely match the desired spectra, improving its design capability. This method, tested with numerous meta-atom configurations and spectrum targets, proves efficient in generating precise meta-filter designs.

Similarly, the paper by Gao et al. [45] introduces a TNN framework for silicon structural color design (Fig. 3b). This network is trained to predict the geometric parameters of silicon nanostructures based on desired color values. In the study by Tanriover et al. [44], the inverse design network for all-dielectric metasurface (Fig. 3c) consists of three components: the H-network, R-network, and forward network. The H-network is tasked with determining the heights of cylindrical meta-atoms based on specific design goals. The R-network, on the other hand, calculates the appropriate radii for these meta-atoms. Finally, the forward network integrates these dimensions to assess the overall optical performance of meta-atoms, ensuring that the designed metasurface meets the targeted optical responses. In the paper by Malkiel et al. [75], the integration of horizontal and vertical spectra, along with material properties, into the architecture of the inverse design network (Fig. 3d) is centered around predicting the far-field optical response for defined nanostructure geometries and compositions. In all of these TNNs, a forward prediction DNN that predicts the responses of meta-atoms is pre-trained and incorporated into the inverse design network. When training the TNNs, the values for all neurons in the forward DNNs are fixed and only the neuron values in the inverse networks are trainable.

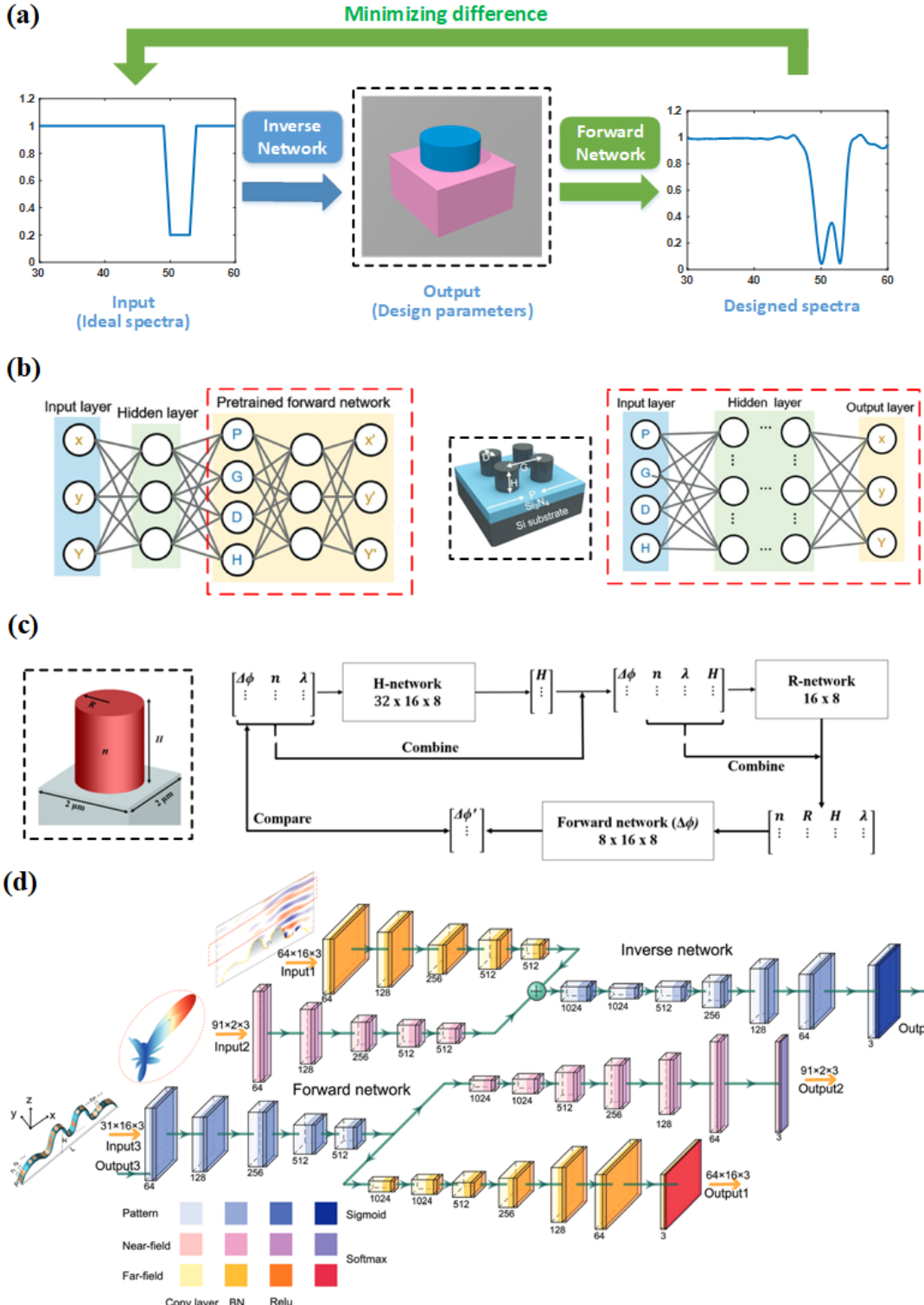


Figure 3. TNNs for the inverse design of metasurfaces. a, a TNN in ref. [17] with target transmission spectra as input and meta-atom design parameters as network output. **b**, a TNN in ref. [45] that generates the design parameters (P , G , D , H) as network output given the target reflection spectra. **c**, a TNN in ref. [44] with design parameters of

cylindrical meta-atoms as network output, given the target phase delay, working wavelength and refractive index as network input. **d**, a TNN in ref. [50] that generates the design of a metasurface cloak.

Recent advancements in the field of metasurface designs have witnessed the emergence of more sophisticated applications of TNNs [27,45,49–53,83]. For instance, He et al. introduced a TNN with a soft constraint to optimize the selection of parameters for designing metasurface absorbers [49]. Concurrently, Wu et al. developed a CNN-based TNN with multiple inputs (Fig. 3d), aimed at generating designs for metasurface cloaks [50]. These advancements highlight the increasing versatility and sophistication of TNNs in addressing diverse challenges in metasurface design, providing more targeted and efficient solutions.

3.3 Autoencoders (AEs)

AEs [102,103] are a type of generative DNNs used primarily for learning efficient representations of data. They work by compressing the input into a latent-space representation and then reconstructing the output from this representation, aiming to match the original input as closely as possible. The network is divided into two parts: the encoder, which compresses the input, and the decoder, which reconstructs the input from the compressed form.

In the context of metasurface design and modeling, autoencoders can be utilized to learn the complex relationships and patterns inherent in metasurface structures. They aid in the compression of high-dimensional data into a lower-dimensional space, making the computational analysis more efficient and manageable [28]. This dimensionality reduction is particularly useful in optimizing the metasurface parameters, generating diverse designs and leading to faster and more accurate performance [32,34,35,39,104–106]. Their ability to reconstruct data also allows for the refinement of metasurface models, potentially leading to more accurate simulations and predictions [20,33,36,107]. Thus, autoencoders offer a versatile and powerful tool for enhancing the capabilities in metasurface design and modeling, combining basic principles of neural networks with the specific needs of this advanced field.

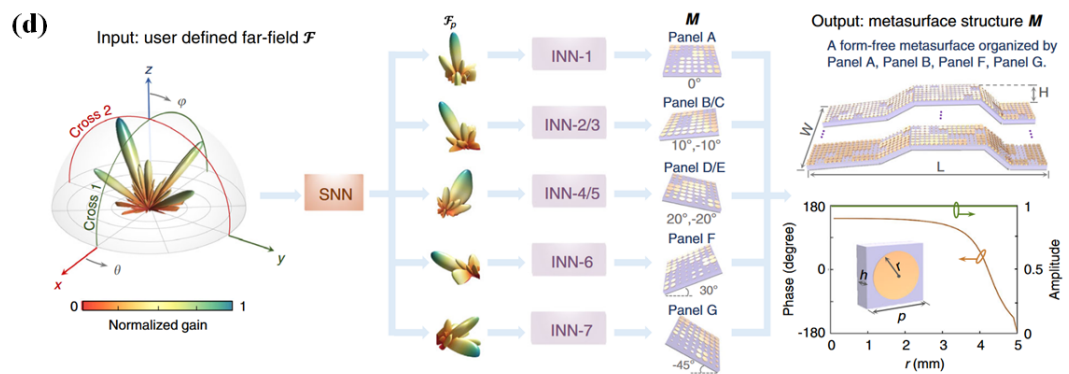
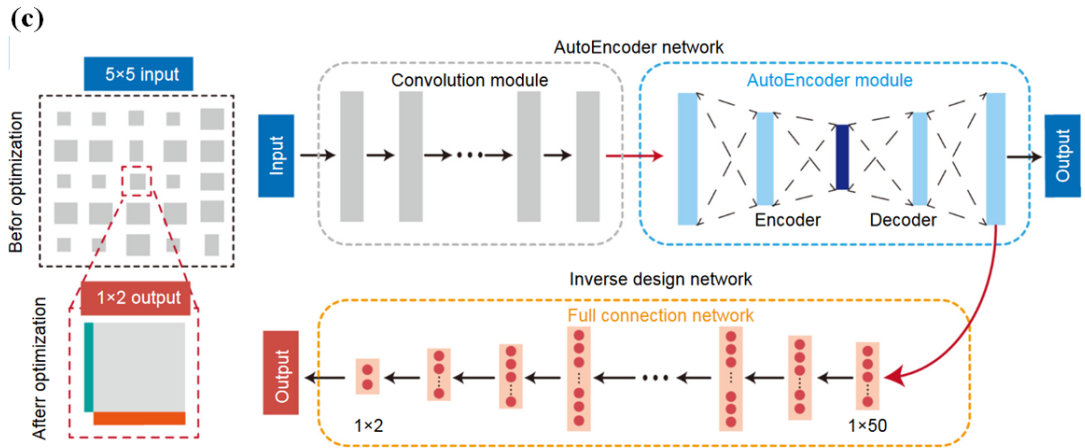
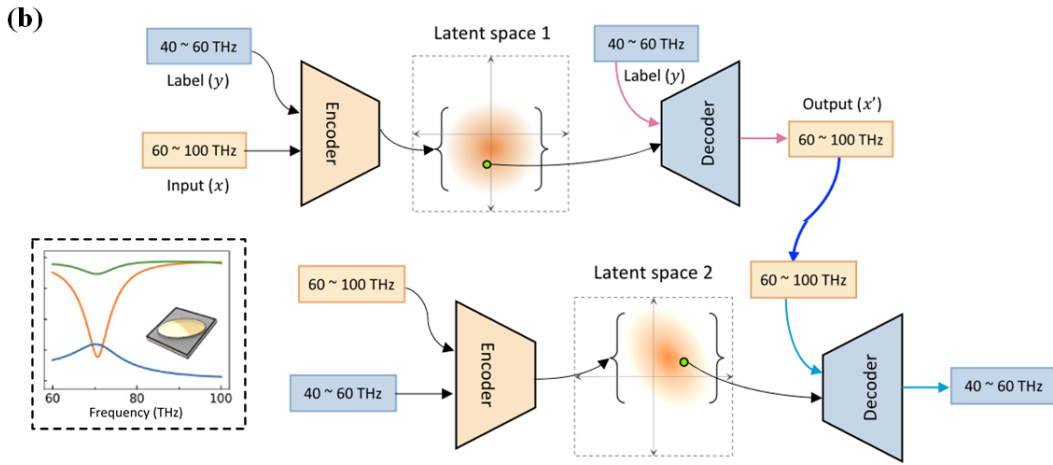
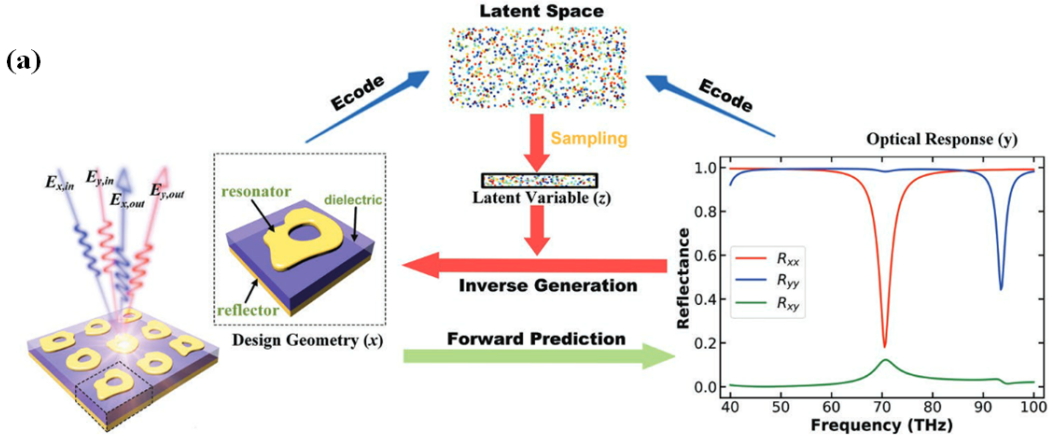


Figure 4. Auto Encoder-Decoder networks for the inverse design of metasurfaces. **a**, an AE model [39] (composed of a recognition model, a prediction model, and a generation model) for metamaterial design and characterization. **b**, an AE model [36] consisting of two cascaded networks (the generation network and the elimination network), each composed of an encoder, the latent space, and a decoder. **c**, an AE model [34] consists of an autoencoder module that expands the information space of sampled data, while the weak coupling strength structures are filtered by the inverse design network. **d**, an AE model [35] contains two encoders (SNN) and one decoder (INN).

Ma et al. [39] presents a novel network architecture for the design of metamaterials. It utilizes a deep generative model with a variational autoencoder (VAE) structure, enabling probabilistic representation of metamaterial designs. This model encodes metamaterial patterns and their optical responses into a latent space, from which new designs satisfying specific requirements can be generated (Fig. 4a). The network is designed to handle both forward prediction and inverse design problems, offering a comprehensive and efficient tool for metamaterial design and characterization. This architecture also employs a semi-supervised learning strategy to improve model performance by utilizing both labeled and unlabeled data. Similarly, Ma and Liu present another VAE to predict and design nanophotonic structures efficiently [104]. The VAE model includes an encoder and a decoder network, both constructed using CNNs and few fully connected layers. The encoder compresses input design patterns into a 20-dimensional latent space, capturing the essential features of the nanophotonic structures. The decoder then reconstructs the input design from the latent variable, sampled from the latent space conditioned on the corresponding reflection spectra. This architecture allows the model to perform both forward prediction of optical responses and inverse design from predetermined metasurface properties.

Ha et al. presents a sophisticated approach to metalens design that integrates physics-based methods with data-driven techniques in a DL framework [34]. This framework (Fig. 4c) consists of two key components: an autoencoder network (A-network) and an inverse design network (I-network). The A-network's role is to efficiently process input data, enhancing the depth of information extraction. This processed data is then utilized by the I-network, which focuses on generating optimized designs for the meta-atoms of the metalenses. The trained AE can adaptively modify the sizes of meta-atoms based on their surrounding ones. Such implementation mitigates the undesired local coupling effect. A centimeter scale metalens with high focusing efficiency was optimized using the fully-trained AE network.

In recent years, the application of autoencoders has expanded significantly within the realm of metasurface design and modeling. Chen et al. used a VAE to infer optical responses from correlated optical responses for metasurface applications [36]. The framework (Fig. 4b) consists of two cascaded networks: a generation network and an elimination network, each comprising an encoder, a latent space, and a decoder. The generation network produces a diverse set of output candidates by sampling over its latent space, while the elimination network selects the optimal candidate by merging two latent spaces and eliminating inferior ones. With the use of these two networks, the study could use low frequency spectra (40 - 60 THz) to predict high frequency (60 – 100 THz) spectra for metasurface. This method overcomes the complex many-to-many mapping challenge, providing a generalized and efficient solution for the prediction and design of metasurface.

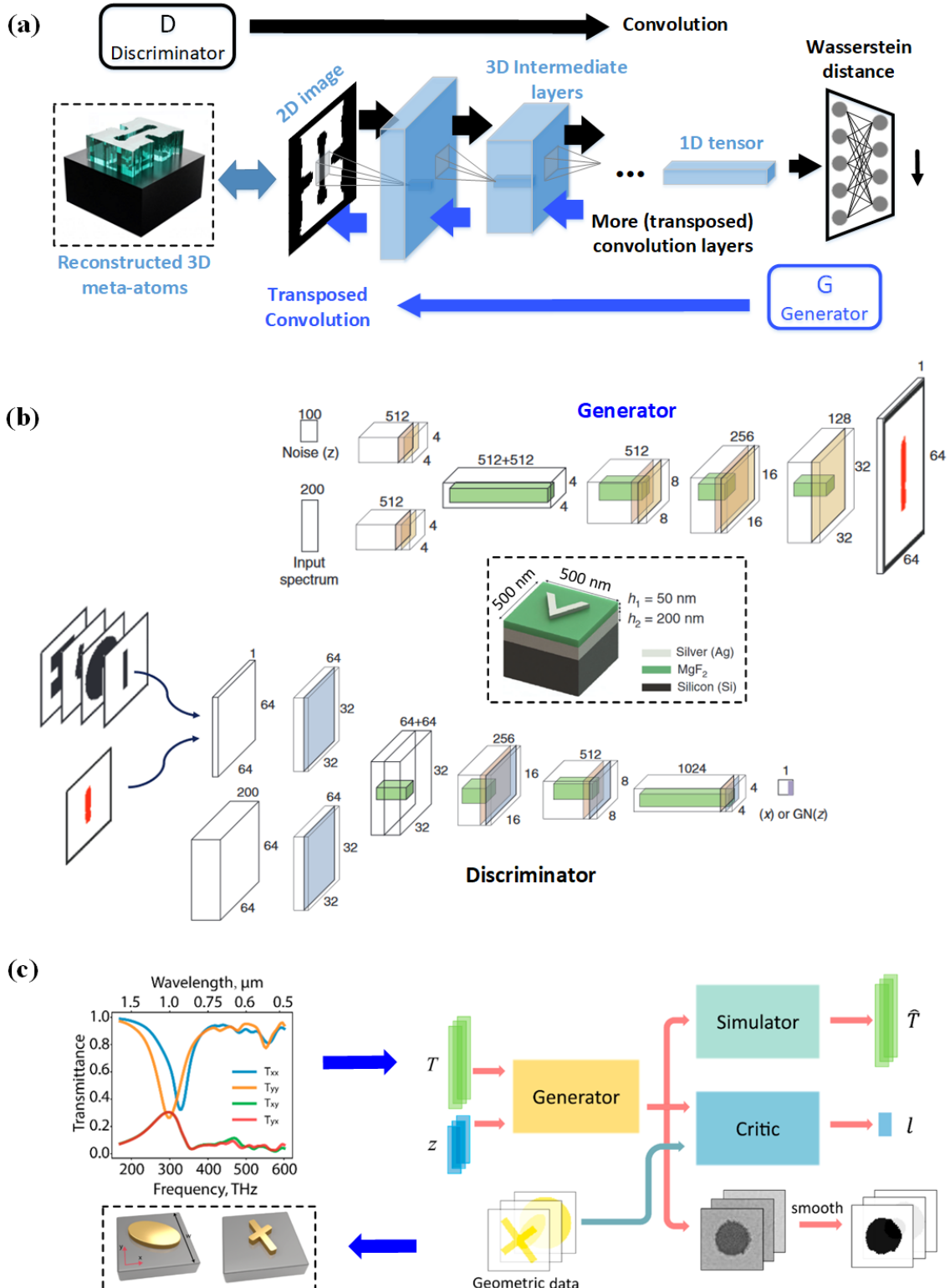
In addition to the spectral responses, Jia et al. focuses on the design of the entire meta-device [35]. The authors developed a unique autoencoder model structure termed as a knowledge-inherited neural network for metasurface design (Fig. 4d). This structure consists of two main parts: an inherited neural network (INN) and an assembled neural network (SNN). The INN is responsible for the inverse design of individual "panel" metasurface, while the SNN functions as a deployer to assign tasks to each INN for constructing a comprehensive "offspring" metasurface. The SNN utilizes an encoder for RCS results and two decoders for the intermediate phase distribution M, and the

real and imaginary parts of the far field. The INN then processes these with two encoders to generate the metasurface design, represented by the phase of four constituting supercells. The innovation lies in the dynamic assembly and flexibility of the network, allowing knowledge from "parent" metasurface to be passed on and combined in novel ways to design "offspring" metasurfaces.

3.4 Generative Adversarial Nets (GANs)

Using TNNs, we can effectively implement the inverse design of simple-shaped meta-atoms, such as cylinders (defined by radius and height) [17,45–47], cubes (length, width, and height) [34,108], and H-shapes (dimensions of each bar and height) [4,17,109–111]. However, TNNs face limitations in generating on-demand designs for more complex meta-atom shapes. Expanding the output tensor in TNNs to encompass a full 2D pattern, representing the cross-section of a free-form meta-atom, and training the network often results in unstable training errors and failure to converge. While EM performance from 2D patterns (large input to small output) for these free-form meta-atoms is relatively straightforward, the inverse process (small input to large output) poses significant challenges. This inverse process, requiring both composition and improvisation of patterns based on targeted EM performances, substantially increases training complexity. On the other hand, AEs are effective for dimensionality reduction and optimization, generating diverse metasurface designs. GANs, however, are uniquely capable of creating complex free-form structures, often exploring beyond the training data distribution to uncover novel design possibilities. This ability to generate innovative and detailed metasurface patterns makes GANs particularly suitable for tasks where the design space is vast and underexplored [112], setting them apart from TNNs and AEs.

GANs [29–31,113] have achieved great success in modeling complex patterns and distributions. Composed of a generator and a discriminator, GANs operate through a competitive dynamic. The generator, often built with deconvolutional layers, expands low-dimensional data into higher dimensions to create new metasurface designs. The discriminator, utilizing convolutional layers, evaluates these designs against real data, distinguishing between authentic and generated designs. Similar to autoencoders, GANs offer transformative potential in metasurface design, especially in inverse design tasks, by enabling the exploration and creation of complex, high-performance structures. This approach is highly beneficial for overcoming limitations in conventional design methods, enhancing the rapid prototyping and development of metasurface models, crucial in the fast-evolving domains of nanophotonics and EM theory [21,38,60–64,114–118].



spectrum. **c**, proposed generative model in ref. [64] consists of a generator, a simulator, and a critic. The trained generator can produce 2D cross sections of gold metasurface on glass.

One significant advantage of GANs is their ability to model the overall distribution of the training data, rather than just memorizing specific datasets. In theory, a fully trained GAN can generate an unlimited number of outputs from the same data distribution. The generator in a GAN uses a latent vector as input, comprising a set of randomly generated, normally distributed values. It transforms this normal distribution into the distribution resembling the real dataset. As a result, even with fixed parameters, the generator can produce diverse outputs. This is a key distinction from tandem inverse design networks, which typically create outputs on a one-to-one basis. An important variant of GANs is the conditional generative adversarial network (CGAN), where the generator produces outputs based on specific input conditions. The discriminator in a CGAN is also conditioned, tasked with determining whether the generated images correspond accurately with the given inputs. This feature enables CGANs to create designs that meet specific targets or belong to certain domains. For instance, by conditioning the target EM responses and using the cross-sections of meta-atoms as input/output images, a CGAN can be trained to generate meta-atom designs tailored to specific EM targets, as shown in Fig. 5a. Utilizing a fully-trained generator, the authors successfully created a variety of effective meta-atom designs with similar performance characteristics [21]. Notably, an analysis of these meta-atoms, generated by the CGAN, has the potential to reveal unique physical characteristics associated with EM responses. Some of these characteristics are readily observable. The neural network processes these designs through several convolutional layers, identifying common traits. These shared features allow the designs to be categorized into the same conditional distribution, a process that is typically non-intuitive and complex. This approach not only streamlines the design process but also deepens our understanding of the physical principles underlying specific EM responses.

The paper by So and Rho [62] employed a conditional deep convolutional generative adversarial network (cDCGAN) to generate free-form silver nanophotonic antennas. The cDCGAN takes input reflection spectra and generates corresponding desirable designs in the form of images (Fig. 5b). In 2018, Liu et al. presented a GAN model utilized for the inverse design of metasurface [64]. The GAN model comprises three key components (Fig. 5c): a generator, a simulator, and a critic. The generator creates metasurface patterns based on input spectra and noise, while the simulator, a pre-trained neural network, approximates the transmissive spectra of these patterns. The critic evaluates the geometric data and the generated patterns, guiding the generator towards realistic designs. This structure allows the GAN to efficiently create diverse and accurate metasurface designs, significantly enhancing the design process of metasurface with tailored optical responses.

More advanced GAN techniques were introduced to assist metasurface inverse design. In the study by Kudyshev et al., the adversarial autoencoder (AAE) [113] is pivotal for optimizing photonic device designs [38]. The AAE operates by encoding design parameters into a compressed representation, which the decoder then attempts to reconstruct. Simultaneously, the discriminator differentiates between real and reconstructed data, refining the model's ability to capture essential design features. This dual process of generation and discrimination underpins the AAE's effectiveness, enhancing its capability to guide the optimization of complex photonic structures by identifying and retaining the most critical design aspects. The application of GANs in metasurface is particularly promising for exploring new design spaces, optimizing existing structures, and generating high-quality, realistic synthetic data for training other machine learning models in this rapidly evolving field.

4. Summary and Discussion

DL Approach	Key Advantages	Disadvantage	Performance Characteristics
FCNNs	<ul style="list-style-type: none"> • Easy implementation • Versatile for various inputs 	<ul style="list-style-type: none"> • Computationally intensive • Prone to overfitting with small data 	<ul style="list-style-type: none"> • High accuracy for simple structures • Memory intensive
2D CNNs	<ul style="list-style-type: none"> • Strong spatial feature extraction • Helps prevent overfitting 	<ul style="list-style-type: none"> • Complex training process • Limited to grid-structured data 	<ul style="list-style-type: none"> • Excellent for complex patterns • Good scalability
Sequential NNs (RNNs/1D CNNs)	<ul style="list-style-type: none"> • Good at processing sequence data • Effective for EM spectrum predictions 	<ul style="list-style-type: none"> • Computationally expensive • Struggle with long data sequences 	<ul style="list-style-type: none"> • Accurate for sequence data • Improve performance on CNN and FCNN
TNNs	<ul style="list-style-type: none"> • Manages non-direct correlations well • Good for designing simple shapes • Stable optimization 	<ul style="list-style-type: none"> • Struggles with complex geometries • Limited variety in outputs 	<ul style="list-style-type: none"> • High accuracy on inverse design • Limited by forward model constraints • Training intensive
AEs	<ul style="list-style-type: none"> • Efficient dimensionality reduction • Great for pulling out important features • Effective for optimization and diverse design generation 	<ul style="list-style-type: none"> • Complex tuning needed • Struggles with high-dimensional inputs • Requires large datasets 	<ul style="list-style-type: none"> • Good at rebuilding data and optimizing • Moderate accuracy on inverse design • Adaptable for high-dimensional data
GANs	<ul style="list-style-type: none"> • Can create multiple solutions • Great design diversity • Handles complex geometries 	<ul style="list-style-type: none"> • Training instability • Demands large computation power • Convergence challenges • Requires large datasets 	<ul style="list-style-type: none"> • High design diversity • Enables exploration of complex distributions • Slow training

Table 2. Advantages and disadvantages of DL method. Columns from left to right: DL methods, advantages, disadvantages and DL performance characteristics.

When deploying DL techniques for metasurface inverse design problems, choosing the right network architecture is crucial for effective training and achieving precise outcomes. Different network architectures and training methods present distinct advantages and challenges (Table 2). Researchers must thoughtfully consider the diverse array of DL approaches in relation to the specifics of the design task, including the complexity of the input/output and the configurations of the data. Making informed decisions on these factors is essential to improve both the efficiency of the training process and the accuracy of the results .

As we venture beyond the overarching narratives of AI's convergence with metasurface technology, it becomes imperative to scrutinize the underlying facts that are pivotal to the maturation of this field. The following subsections

synthesize the key insights from our exploration, highlighting how advanced DL techniques are revolutionizing metasurface design and modeling.

4.1 Data collection

In the area of metasurface design and modeling, a key factor enhancing the effectiveness of DL models is the process of data collection. Many previous studies have relied on large datasets, often comprising hundreds of thousands of spectral data points, to train DL models. This approach, while effective in achieving accuracy, can be time-consuming due to the substantial demands of simulation. However, the nature and properties of the training data are often overlooked. As Dong et al. [87] pointed out, the success of DL in this domain heavily relies on the quality, diversity, and size of the dataset. A comprehensive and varied dataset, encompassing a wide range of design parameters and EM responses, is crucial for developing robust and precise models.

In their study, Dong et al. gathered two large datasets for training a model to predict the spectrum of all-dielectric meta-atoms. One dataset, although large (30,000 meta-atoms), was significantly unbalanced. They employed a data sampling method to balance this dataset, reducing its size to 15,000 samples while maintaining its representativeness. This balanced approach led to notable improvements: the model trained with the larger, unbalanced dataset achieved a mean absolute error (MAE) of 0.134, while the model trained with the balanced, smaller dataset significantly outperformed it, achieving an MAE of 0.079. The contrast in performance between the models trained on the larger, unbalanced dataset and the smaller, balanced dataset underscores a crucial insight: the quality and representativeness of training data can be more influential than sheer volume. Therefore, the balance of quality and quantity in data collection is a key determinant factor in the successful deployment of DL techniques in the intricate field of metasurface design and modeling.

4.2 Choosing different inverse DL models

Advanced inverse models like AEs, GANs, and TNNs each have distinct advantages. TNNs and VAEs generally offer higher accuracy in metasurface design, but TNNs may face challenges with specific tasks when requiring multiple alternative structures. In contrast, generative models like VAEs and GANs can offer multiple predictions, enhancing versatility. Notably, GANs are distinguished by their diverse, multi-modal outputs, offering designers a variety of choices for optimal structures [112]. Thus, when confronted with metasurface model or design problems, the selection of these methods should be carefully aligned with the specific requirements of the task at hand.

4.3 AI for fabrication-friendly metasurfaces

Performance of metasurfaces can deteriorate from design to manufacturing due to unavoidable geometric variations from fabrication errors, particularly in complex subwavelength structures. Geometric deviations like edge roughness are often uncontrollable, whereas issues like structure erosion or dilation arise from dosing and etching processes and can be systematically managed. Although precise fabrication of tight-tolerance structures is possible, it increases costs related to the process window - the acceptable manufacturing parameters range. Structures less sensitive to process variations are preferred for wider manufacturing windows, reducing costs and improving yield. With the help of AI, suitable selection of meta-atoms can be quickly generated from the pool of meta-atoms derived with inverse design DNNs [56,89]. As for future directions, it would be interesting to train DNN models to generalize across various types of fabrication errors such as edge roughness and side wall angles [119].

4.4 AI for reconfigurable metasurface design

Active metasurfaces, compared to traditional ones, allow for advanced manipulation of dispersion characteristics, surpassing the capabilities of homogeneous material layers. However, designing these metasurfaces is computationally demanding due to the extensive degrees of freedom in free-form meta-atom geometries and the range of tunable material states. DNNs offer a promising solution to these complex photonic design challenges. In [19], the authors demonstrate that DNNs can predict and inversely design broadband complex S-parameters of active metasurface elements. These DNNs, combined with the transfer matrix method (TMM) for analytical optimization, enhance the efficient design of metasurfaces-embedded tunable photonic devices. A notable application is the design of an actively tunable optical bandpass filter, integrating a phase change material (PCM) metasurface with two distributed Bragg reflectors (DBRs), operational in the mid-wave infrared (MWIR) waveband. The authors developed a forward prediction DNN for rapid and precise evaluation of meta-atoms across various crystallization states, alongside an inverse design DNN, based on TNN architecture, for creating on-demand designs from target transmission spectra under different states. The effectiveness of this DNN framework is showcased through several filter designs operating at MWIR.

A similar design framework based on DNNs was introduced in [17] to find the optimal meta-atom design with maximum phase coverage constructed with phase change materials. This DNN-generated design achieves over 320 degrees of phase coverage, with the meta-atom transitioning between states. In its amorphous state (material index of 3.57), it supports an electric dipole resonance, while in the crystalline state (index of 4.15), it exhibits a strong magnetic dipole moment. These alternating resonances are key for achieving full 2π phase coverage. The network efficiently pinpoints design parameters within minutes, showcasing a significant improvement over traditional methods that require extensive parameter sweeps and analysis.

4.5 Other challenges on DL in metasurface design

The implementation of DL in metasurface design faces several significant practical challenges that researchers are actively working to address. As we review the current landscape of DL applications in this field, we observe several trends addressing these challenges:

1. Large Labeled Datasets: The requirement for extensive labeled data, typically obtained through time EM simulations, presents a major hurdle. Researchers are mitigating this challenge by exploring various strategies, including the use of transfer learning techniques to leverage pre-trained models [70], and advanced data sampling methods [87]. These approaches help in maximizing the utility of available data and reducing the need for extensive simulations.

2. Interpretability of DL Models: Enhancing model transparency remains a critical focus. Developments in physically informed networks [72] aim to integrate physical principles directly into DL models, facilitating the extraction of physically meaningful features. This approach helps bridge the gap between the unclear 'black-box' nature of traditional DL models and the need for understandable, reliable predictions. Looking forward, the future development of visualization techniques to interpret network decisions and methods for extracting design rules from trained models is also anticipated.

3. Computational costs: The computational demands associated with training and implementing DL models pose practical limitations. These challenges are being addressed by optimizing network architectures, developing surrogate models to expedite training [88], and employing distributed training strategies [116]. These methods enhance the efficiency of computational resources and reduce training times.

4.6 DL assisted real-world metasurface application

Although most published works only validate their DL models through numerical simulations, in recent years, several studies [43,51,56,120] have successfully demonstrated practical implementations of DL-designed metasurfaces. These successful examples have shown how DL models can effectively address real-world metasurface design challenges by accelerating the design process, enabling multifunctional, complex structures, optimizing fabrication constraints, and exploring novel design possibilities that would be difficult to achieve through conventional methods. For instance, in ref. [56], a CNN based neural network has been used to make the forward prediction of free-form meta-atoms' EM responses. Then the author uses this network to fast select meta-atoms from the library that meet fabrication friendly requirement. Finally, the selected meta-atoms were used to design dual-band optical collimators with focal length of 15mm, achieving precise beam collimation at two wavelengths (650 nm and 780 nm), which is practical for optical communication and laser beam shaping. In another work [120], the proposed Adaptive Tandem network integrates spatial and spectral attention mechanisms to synthesize metasurface polarizers capable of linear polarization to both orthogonal linear polarization (LP-OLP) and circular polarization (LP-CP) across two frequency bands. The inverse design network was then used to design a dual-band dual-polarization converter. The fabricated prototype includes 20×20 metasurface unit cells. The structure maintains stable performance up to an oblique incidence angle of 10° , demonstrating its reliability and practicality for real-world applications. These successful implementations demonstrate that deep learning approaches have matured beyond theoretical concepts to become practical tools for real-world metasurface design and optimization.

5. Conclusion

In this review, we provided an in-depth exploration of the application of DL in the field of metasurface design and modeling within nanophotonic engineering, indicative of the rapid advancements in this area. The implementation of sophisticated DL methodologies, such as AEs, TNNs, and GANs, is congruent with the latest trends in the engineering of metasurface devices. These advanced DL techniques markedly streamline the processes of inverse design.

To conclude, the intersection of AI and DL with metasurface technology is an emerging and promising area of research. As discussed throughout this paper, this intersection holds the potential to facilitate new research directions aimed at enhancing the precision and functionality of metasurface devices. Future research is expected to explore additional applications and techniques to further the development of DL implementations of metasurface design and modeling.

Acknowledgments

This research was supported by the National Science Foundation (Grant #: 2132929) and Defense Advanced Research Projects Agency (Grant #: HR00111720029, HR00112290005).

Reference

- [1] M. Khorasaninejad, Z. Shi, A.Y. Zhu, W.T. Chen, V. Sanjeev, A. Zaidi, F. Capasso, Achromatic Metalens over 60 nm Bandwidth in the Visible and Metalens with Reverse Chromatic Dispersion, *Nano Lett.* 17 (2017) 1819–1824. <https://doi.org/10.1021/acs.nanolett.6b05137>.
- [2] A. Arbabi, Y. Horie, M. Bagheri, A. Faraon, Dielectric metasurfaces for complete control of phase and polarization with subwavelength spatial resolution and high transmission, *Nat. Nanotechnol.* 10 (2015) 937–943. <https://doi.org/10.1038/nnano.2015.186>.
- [3] X. Ni, N.K. Emani, A.V. Kildishev, A. Boltasseva, V.M. Shalaev, Broadband Light Bending with Plasmonic Nanoantennas, *Science* 335 (2012) 427–427. <https://doi.org/10.1126/science.1214686>.
- [4] L. Zhang, J. Ding, H. Zheng, S. An, H. Lin, B. Zheng, Q. Du, G. Yin, J. Michon, Y. Zhang, Z. Fang, M.Y. Shalaginov, L. Deng, T. Gu, H. Zhang, J. Hu, Ultra-thin high-efficiency mid-infrared transmissive Huygens meta-optics, *Nat. Commun.* 9 (2018) 1481. <https://doi.org/10.1038/s41467-018-03831-7>.
- [5] Z.-B. Fan, H.-Y. Qiu, H.-L. Zhang, X.-N. Pang, L.-D. Zhou, L. Liu, H. Ren, Q.-H. Wang, J.-W. Dong, A broadband achromatic metalens array for integral imaging in the visible, *Light Sci. Appl.* 8 (2019) 67. <https://doi.org/10.1038/s41377-019-0178-2>.
- [6] W. Ma, Z. Liu, Z.A. Kudyshev, A. Boltasseva, W. Cai, Y. Liu, Deep learning for the design of photonic structures, *Nat. Photonics* 15 (2021) 77–90. <https://doi.org/10.1038/s41566-020-0685-y>.
- [7] A. Khaireh-Walieh, D. Langevin, P. Bennet, O. Teytaud, A. Moreau, P.R. Wiecha, A newcomer’s guide to deep learning for inverse design in nano-photonics, *Nanophotonics* 12 (2023) 4387–4414. <https://doi.org/10.1515/nanoph-2023-0527>.
- [8] C.-X. Liu, G.-L. Yu, Deep learning for the design of phononic crystals and elastic metamaterials, *J. Comput. Des. Eng.* 10 (2023) 602–614. <https://doi.org/10.1093/jcde/qwad013>.
- [9] L. He, Y. Li, D. Torrent, X. Zhuang, T. Rabczuk, Y. Jin, Machine learning assisted intelligent design of meta structures: a review, *Microstructures* 3 (2023). <https://doi.org/10.20517/microstructures.2023.29>.
- [10] W. Ji, J. Chang, H.-X. Xu, J.R. Gao, S. Gröblacher, H.P. Urbach, A.J.L. Adam, Recent advances in metasurface design and quantum optics applications with machine learning, physics-informed neural networks, and topology optimization methods, *Light Sci. Appl.* 12 (2023) 169. <https://doi.org/10.1038/s41377-023-01218-y>.
- [11] V. Sze, Y.-H. Chen, T.-J. Yang, J.S. Emer, Efficient Processing of Deep Neural Networks: A Tutorial and Survey, *Proc. IEEE* 105 (2017) 2295–2329. <https://doi.org/10.1109/JPROC.2017.2761740>.
- [12] G. Montavon, W. Samek, K.-R. Müller, Methods for interpreting and understanding deep neural networks, *Digit. Signal Process.* 73 (2018) 1–15. <https://doi.org/10.1016/j.dsp.2017.10.011>.
- [13] J.N. Kutz, Deep learning in fluid dynamics, *J. Fluid Mech.* 814 (2017) 1–4. <https://doi.org/10.1017/jfm.2016.803>.
- [14] K. Ryan, J. Lengyel, M. Shatruk, Crystal Structure Prediction via Deep Learning, *J. Am. Chem. Soc.* 140 (2018) 10158–10168. <https://doi.org/10.1021/jacs.8b03913>.
- [15] K. Sato, M. Akiyama, Y. Sakakibara, RNA secondary structure prediction using deep learning with thermodynamic integration, *Nat. Commun.* 12 (2021) 941. <https://doi.org/10.1038/s41467-021-21194-4>.
- [16] Y.H. Kan, C.Y. Zhao, Z.M. Zhang, Enhancement and Manipulation of Near-Field Radiative Heat Transfer Using an Intermediate Modulator, *Phys. Rev. Appl.* 13 (2020) 014069. <https://doi.org/10.1103/PhysRevApplied.13.014069>.
- [17] S. An, C. Fowler, B. Zheng, M.Y. Shalaginov, H. Tang, H. Li, L. Zhou, J. Ding, A.M. Agarwal, C. Rivero-Baleine, K.A. Richardson, T. Gu, J. Hu, H. Zhang, A Deep Learning Approach for Objective-Driven All-Dielectric Metasurface Design, *ACS Photonics* 6 (2019) 3196–3207. <https://doi.org/10.1021/acsphotonics.9b00966>.
- [18] S. An, B. Zheng, M.Y. Shalaginov, H. Tang, H. Li, L. Zhou, Y. Dong, M. Haerinia, A.M. Agarwal, C. Rivero-Baleine, M. Kang, K.A. Richardson, T. Gu, J. Hu, C. Fowler, H. Zhang, Deep Convolutional Neural

Networks to Predict Mutual Coupling Effects in Metasurfaces, *Adv. Opt. Mater.* 10 (2022) 2102113. <https://doi.org/10.1002/adom.202102113>.

[19] S. An, B. Zheng, M. Julian, C. Williams, H. Tang, T. Gu, H. Zhang, H.J. Kim, J. Hu, Deep neural network enabled active metasurface embedded design, *Nanophotonics* 11 (2022) 4149–4158. <https://doi.org/10.1515/nanoph-2022-0152>.

[20] P.R. Wiecha, O.L. Muskens, Deep Learning Meets Nanophotonics: A Generalized Accurate Predictor for Near Fields and Far Fields of Arbitrary 3D Nanostructures, *Nano Lett.* 20 (2020) 329–338. <https://doi.org/10.1021/acs.nanolett.9b03971>.

[21] S. An, B. Zheng, H. Tang, M.Y. Shalaginov, L. Zhou, H. Li, M. Kang, K.A. Richardson, T. Gu, J. Hu, C. Fowler, H. Zhang, Multifunctional Metasurface Design with a Generative Adversarial Network, *Adv. Opt. Mater.* 9 (2021) 2001433. <https://doi.org/10.1002/adom.202001433>.

[22] Y. Zhang, J. Lee, M. Wainwright, M.I. Jordan, On the learnability of fully-connected neural networks, in: A. Singh, J. Zhu (Eds.), *Proc. 20th Int. Conf. Artif. Intell. Stat.*, PMLR, 2017: pp. 83–91. <https://proceedings.mlr.press/v54/zhang17a.html>.

[23] S.H.S. Basha, S.R. Dubey, V. Pulabaigari, S. Mukherjee, Impact of fully connected layers on performance of convolutional neural networks for image classification, *Neurocomputing* 378 (2020) 112–119. <https://doi.org/10.1016/j.neucom.2019.10.008>.

[24] K. Simonyan, A. Zisserman, Very deep convolutional networks for large-scale image recognition, in: *3rd Int. Conf. Learn. Represent. ICLR 2015*, Computational and Biological Learning Society, 2015: pp. 1–14.

[25] M.D. Zeiler, R. Fergus, Visualizing and Understanding Convolutional Networks, in: D. Fleet, T. Pajdla, B. Schiele, T. Tuytelaars (Eds.), *Comput. Vis. – ECCV 2014*, Springer International Publishing, Cham, 2014: pp. 818–833.

[26] K. He, X. Zhang, S. Ren, J. Sun, Deep Residual Learning for Image Recognition, (2015). <https://doi.org/10.48550/arXiv.1512.03385>.

[27] D. Liu, Y. Tan, E. Khoram, Z. Yu, Training Deep Neural Networks for the Inverse Design of Nanophotonic Structures, *ACS Photonics* 5 (2018) 1365–1369. <https://doi.org/10.1021/acsphotonics.7b01377>.

[28] Y. Wang, H. Yao, S. Zhao, Auto-encoder based dimensionality reduction, *RoLoD Robust Local Descr. Comput. Vis.* 2014 184 (2016) 232–242. <https://doi.org/10.1016/j.neucom.2015.08.104>.

[29] I. Goodfellow, J. Pouget-Abadie, M. Mirza, B. Xu, D. Warde-Farley, S. Ozair, A. Courville, Y. Bengio, Generative Adversarial Nets, in: Z. Ghahramani, M. Welling, C. Cortes, N. Lawrence, K.Q. Weinberger (Eds.), *Adv. Neural Inf. Process. Syst.*, Curran Associates, Inc., 2014. https://proceedings.neurips.cc/paper_files/paper/2014/file/5ca3e9b122f61f8f06494c97b1afccf3-Paper.pdf.

[30] M. Mirza, S. Osindero, Conditional generative adversarial nets, *ArXiv Prepr. ArXiv14111784* (2014).

[31] M. Arjovsky, S. Chintala, L. Bottou, Wasserstein Generative Adversarial Networks, in: D. Precup, Y.W. Teh (Eds.), *Proc. 34th Int. Conf. Mach. Learn.*, PMLR, 2017: pp. 214–223. <https://proceedings.mlr.press/v70/arjovsky17a.html>.

[32] M.K. Chen, X. Liu, Y. Wu, J. Zhang, J. Yuan, Z. Zhang, D.P. Tsai, A Meta-Device for Intelligent Depth Perception, *Adv. Mater.* 35 (2023) 2107465. <https://doi.org/10.1002/adma.202107465>.

[33] M. Zandehshahvar, Y. Kiarashi, M. Zhu, D. Bao, M. H Javani, R. Pourabolghasem, A. Adibi, Metric Learning: Harnessing the Power of Machine Learning in Nanophotonics, *ACS Photonics* (2023) acsphotonics.2c01331. <https://doi.org/10.1021/acsphotonics.2c01331>.

[34] Y. Ha, Y. Luo, M. Pu, F. Zhang, Q. He, J. Jin, M. Xu, Y. Guo, X. Li, X. Li, X. Ma, X. Luo, National Key Laboratory of Optical Field Manipulation Science and Technology, Chinese Academy of Sciences, Chengdu 610209, China, State Key Laboratory of Optical Technologies on Nano-Fabrication and Micro-Engineering, Institute of Optics and Electronics, Chinese Academy of Sciences, Chengdu 610209, China, Research Center on Vector Optical Fields, Institute of Optics and Electronics, Chinese Academy of Sciences, Chengdu 610209, China, School of Optoelectronics, University of Chinese Academy of Sciences, Beijing 100049, China, Tianfu Xinglong Lake Laboratory, Chengdu 610299, China, Physics-data-driven intelligent optimization for large-aperture metalenses, *Opto-Electron. Adv.* 6 (2023) 230133–230133. <https://doi.org/10.29026/oea.2023.230133>.

[35] Y. Jia, C. Qian, Z. Fan, T. Cai, E.-P. Li, H. Chen, A knowledge-inherited learning for intelligent metasurface design and assembly, *Light Sci. Appl.* 12 (2023) 82. <https://doi.org/10.1038/s41377-023-01131-4>.

[36] J. Chen, C. Qian, J. Zhang, Y. Jia, H. Chen, Correlating metasurface spectra with a generation-elimination framework, *Nat. Commun.* 14 (2023) 4872. <https://doi.org/10.1038/s41467-023-40619-w>.

[37] R. Zhu, J. Wang, T. Qiu, D. Yang, B. Feng, Z. Chu, T. Liu, Y. Han, H. Chen, S. Qu, Shaanxi Key Laboratory of Artificially-Structured Functional Materials and Devices, Air Force Engineering University, Xi'an 710051, China, The Academy for Engineering & Technology, Fudan University, Shanghai 200433, China, Direct field-to-pattern monolithic design of holographic metasurface via residual encoder-decoder convolutional neural network, *Opto-Electron. Adv.* 6 (2023) 220148–220148. <https://doi.org/10.29026/oea.2023.220148>.

[38] Z.A. Kudyshev, A.V. Kildishev, V.M. Shalaev, A. Boltasseva, Machine learning-assisted global optimization of photonic devices, *Nanophotonics* 10 (2020) 371–383. <https://doi.org/10.1515/nanoph-2020-0376>.

[39] W. Ma, F. Cheng, Y. Xu, Q. Wen, Y. Liu, Probabilistic Representation and Inverse Design of Metamaterials Based on a Deep Generative Model with Semi-Supervised Learning Strategy, *Adv. Mater.* 31 (2019) 1901111. <https://doi.org/10.1002/adma.201901111>.

[40] T. Knightley, A. Yakovlev, V. Pacheco-Peña, Neural Network Design of Multilayer Metamaterial for Temporal Differentiation, *Adv. Opt. Mater.* 11 (2023) 2202351. <https://doi.org/10.1002/adom.202202351>.

[41] S. Gladyshev, T.D. Karamanos, L. Kuhn, D. Beutel, T. Weiss, C. Rockstuhl, A. Bogdanov, Inverse design of all-dielectric metasurfaces with accidental bound states in the continuum, *Nanophotonics* 12 (2023) 3767–3779. <https://doi.org/10.1515/nanoph-2023-0373>.

[42] O. Yesilyurt, S. Peana, V. Mkhitaryan, K. Pagadala, V.M. Shalaev, A.V. Kildishev, A. Boltasseva, Fabrication-conscious neural network based inverse design of single-material variable-index multilayer films, *Nanophotonics* 12 (2023) 993–1006. <https://doi.org/10.1515/nanoph-2022-0537>.

[43] H. Baali, M. Addouche, A. Bouzerdoum, A. Khelif, Design of acoustic absorbing metasurfaces using a data-driven approach, *Commun. Mater.* 4 (2023) 40. <https://doi.org/10.1038/s43246-023-00369-0>.

[44] I. Tanriover, W. Hadibrata, K. Aydin, A Physics Based Approach for Neural Networks Enabled Design of All-Dielectric Metasurfaces, (n.d.).

[45] L. Gao, X. Li, D. Liu, L. Wang, Z. Yu, A Bidirectional Deep Neural Network for Accurate Silicon Color Design, *Adv. Mater.* 31 (2019) 1905467. <https://doi.org/10.1002/adma.201905467>.

[46] K.-F. Lin, C.-C. Hsieh, S.-C. Hsin, W.-F. Hsieh, Achieving high numerical aperture near-infrared imaging based on an ultrathin cylinder dielectric metalens, *Appl. Opt.* 58 (2019) 8914. <https://doi.org/10.1364/AO.58.008914>.

[47] X. Li, J. Shu, W. Gu, L. Gao, Deep neural network for plasmonic sensor modeling, *Opt. Mater. Express* 9 (2019) 3857. <https://doi.org/10.1364/OME.9.003857>.

[48] J. Peurifoy, Y. Shen, L. Jing, Y. Yang, F. Cano-Renteria, B.G. DeLacy, J.D. Joannopoulos, M. Tegmark, M. Solja, Nanophotonic particle simulation and inverse design using artificial neural networks, *Sci. Adv.* (2018).

[49] X. He, X. Cui, C.T. Chan, Constrained tandem neural network assisted inverse design of metasurfaces for microwave absorption, *Opt. Express* 31 (2023) 40969. <https://doi.org/10.1364/OE.506936>.

[50] N. Wu, Y. Jia, C. Qian, H. Chen, Pushing the Limits of Metasurface Cloak Using Global Inverse Design, *Adv. Opt. Mater.* 11 (2023) 2202130. <https://doi.org/10.1002/adom.202202130>.

[51] H. Xie, X. Yue, K. Wen, D. Liang, T. Han, L. Deng, Deep-learning based broadband reflection reduction metasurface, *Opt. Express* 31 (2023) 14593. <https://doi.org/10.1364/OE.486096>.

[52] S. Sarkar, A. Ji, Z. Jermain, R. Lipton, M. Brongersma, K. Dayal, H.Y. Noh, Physics-Informed Machine Learning for Inverse Design of Optical Metamaterials, *Adv. Photonics Res.* 4 (2023) 2300158. <https://doi.org/10.1002/adpr.202300158>.

[53] X. Xu, C. Sun, Y. Li, J. Zhao, J. Han, W. Huang, An improved tandem neural network for the inverse design of nanophotonics devices, *Opt. Commun.* 481 (2021) 126513. <https://doi.org/10.1016/j.optcom.2020.126513>.

[54] Z. Deng, Y. Li, Y. Li, Y. Wang, W. Li, Z. Zhu, C. Guan, J. Shi, Diverse ranking metamaterial inverse design based on contrastive and transfer learning, *Opt. Express* 31 (2023) 32865. <https://doi.org/10.1364/OE.502006>.

[55] Z. Zeng, L. Wang, Y. Wu, Z. Hu, J. Evans, X. Zhu, G. Ye, S. He, Utilizing Mixed Training and Multi-Head Attention to Address Data Shift in AI-Based Electromagnetic Solvers for Nano-Structured Metamaterials, *Nanomaterials* 13 (2023) 2778. <https://doi.org/10.3390/nano13202778>.

[56] A. Ueno, H.-I. Lin, F. Yang, S. An, L. Martin-Monier, M.Y. Shalaginov, T. Gu, J. Hu, Dual-band optical collimator based on deep-learning designed, fabrication-friendly metasurfaces, *Nanophotonics* 12 (2023) 3491–3499. <https://doi.org/10.1515/nanoph-2023-0329>.

[57] Z. Liu, Z. Dang, Z. Liu, Y. Li, X. He, Y. Dai, Y. Chen, P. Peng, Z. Fang, Self-design of arbitrary polarization-control waveplates via deep neural networks, *Photonics Res.* 11 (2023) 695. <https://doi.org/10.1364/PRJ.480845>.

[58] S. An, B. Zheng, M.Y. Shalaginov, H. Tang, H. Li, L. Zhou, J. Ding, A.M. Agarwal, C. Rivero-Baleine, M. Kang, K.A. Richardson, T. Gu, J. Hu, C. Fowler, H. Zhang, Deep learning modeling approach for metasurfaces with high degrees of freedom, *Opt. Express* 28 (2020) 31932. <https://doi.org/10.1364/OE.401960>.

[59] I. Sajedian, J. Kim, J. Rho, Finding the optical properties of plasmonic structures by image processing using a combination of convolutional neural networks and recurrent neural networks, *Microsyst. Nanoeng.* 5 (2019) 27. <https://doi.org/10.1038/s41378-019-0069-y>.

[60] H.P. Wang, D.M. Cao, X.Y. Pang, X.H. Zhang, S.Y. Wang, W.Y. Hou, C.C. Nie, Y.B. Li, Inverse design of metasurfaces with customized transmission characteristics of frequency band based on generative adversarial networks, *Opt. Express* 31 (2023) 37763. <https://doi.org/10.1364/OE.503139>.

[61] P. Dai, K. Sun, X. Yan, O.L. Muskens, C.H. (Kees) De Groot, X. Zhu, Y. Hu, H. Duan, R. Huang, Inverse design of structural color: finding multiple solutions *via* conditional generative adversarial networks, *Nanophotonics* 11 (2022) 3057–3069. <https://doi.org/10.1515/nanoph-2022-0095>.

[62] S. So, J. Rho, Designing nanophotonic structures using conditional deep convolutional generative adversarial networks, *Nanophotonics* 8 (2019) 1255–1261. <https://doi.org/10.1515/nanoph-2019-0117>.

[63] J. Jiang, D. Sell, S. Hoyer, J. Hickey, J. Yang, J.A. Fan, Free-Form Diffractive Metagrating Design Based on Generative Adversarial Networks, *ACS Nano* 13 (2019) 8872–8878. <https://doi.org/10.1021/acsnano.9b02371>.

[64] Z. Liu, D. Zhu, S.P. Rodrigues, K.-T. Lee, W. Cai, Generative Model for the Inverse Design of Metasurfaces, *Nano Lett.* 18 (2018) 6570–6576. <https://doi.org/10.1021/acs.nanolett.8b03171>.

[65] X. Han, Z. Fan, Z. Liu, C. Li, L.J. Guo, Inverse design of metasurface optical filters using deep neural network with high degrees of freedom, *InfoMat* 3 (2021) 432–442. <https://doi.org/10.1002/inf2.12116>.

[66] S. An, B. Zheng, M.Y. Shalaginov, H. Tang, H. Li, L. Zhou, M. Haerinia, Y. Dong, A.M. Agarwal, C. Rivero-Baleine, M. Kang, K.A. Richardson, T. Gu, J. Hu, C. Fowler, H. Zhang, A Deep Learning Approach to Explore the Mutual Coupling Effects in Metasurfaces, in: Conf. Lasers Electro-Opt., Optica Publishing Group, San Jose, California, 2021: p. JTU3A.75. https://doi.org/10.1364/CLEO_AT.2021.JTU3A.75.

[67] Z. Liu, D. Zhu, K. Lee, A.S. Kim, L. Raju, W. Cai, Compounding Meta-Atoms into Metamolecules with Hybrid Artificial Intelligence Techniques, *Adv. Mater.* 32 (2020) 1904790. <https://doi.org/10.1002/adma.201904790>.

[68] L. Gao, Y. Qu, L. Wang, Z. Yu, Computational spectrometers enabled by nanophotonics and deep learning, *Nanophotonics* 11 (2022) 2507–2529. <https://doi.org/10.1515/nanoph-2021-0636>.

[69] D. Ma, Z. Li, W. Liu, G. Geng, H. Cheng, J. Li, J. Tian, S. Chen, Deep-Learning Enabled Multicolor Meta-Holography, *Adv. Opt. Mater.* 10 (2022) 2102628. <https://doi.org/10.1002/adom.202102628>.

[70] J. Zhang, C. Qian, Z. Fan, J. Chen, E. Li, J. Jin, H. Chen, Heterogeneous Transfer-Learning-Enabled Diverse Metasurface Design, *Adv. Opt. Mater.* 10 (2022) 2200748. <https://doi.org/10.1002/adom.202200748>.

[71] L. Kuhn, T. Repän, C. Rockstuhl, Inverse design of core-shell particles with discrete material classes using neural networks, *Sci. Rep.* 12 (2022) 19019. <https://doi.org/10.1038/s41598-022-21802-3>.

[72] O. Khatib, S. Ren, J. Malof, W.J. Padilla, Learning the Physics of All-Dielectric Metamaterials with Deep Lorentz Neural Networks, *Adv. Opt. Mater.* 10 (2022) 2200097. <https://doi.org/10.1002/adom.202200097>.

[73] H. Wei, H. Bao, X. Ruan, Perspective: Predicting and optimizing thermal transport properties with machine learning methods, *Energy AI* 8 (2022) 100153. <https://doi.org/10.1016/j.egyai.2022.100153>.

[74] Y. Chen, L. Dal Negro, Physics-informed neural networks for imaging and parameter retrieval of photonic nanostructures from near-field data, *APL Photonics* 7 (2022) 010802. <https://doi.org/10.1063/5.0072969>.

[75] I. Malkiel, M. Mrejen, A. Nagler, U. Arieli, L. Wolf, H. Suchowski, Plasmonic nanostructure design and characterization via Deep Learning, *Light Sci. Appl.* 7 (2018) 60. <https://doi.org/10.1038/s41377-018-0060-7>.

[76] S. So, J. Mun, J. Rho, Simultaneous Inverse Design of Materials and Structures via Deep Learning: Demonstration of Dipole Resonance Engineering Using Core–Shell Nanoparticles, *ACS Appl. Mater. Interfaces* 11 (2019) 24264–24268. <https://doi.org/10.1021/acsami.9b05857>.

[77] Z. Liu, Z. Zhu, W. Cai, Topological encoding method for data-driven photonics inverse design, *Opt. Express* 28 (2020) 4825. <https://doi.org/10.1364/OE.387504>.

[78] F. Wang, G. Geng, X. Wang, J. Li, Y. Bai, J. Li, Y. Wen, B. Li, J. Sun, J. Zhou, Visible Achromatic Metalens Design Based on Artificial Neural Network, *Adv. Opt. Mater.* 10 (2022) 2101842. <https://doi.org/10.1002/adom.202101842>.

[79] S. Noureen, M. Zubair, M. Ali, M.Q. Mehmood, Deep learning based hybrid sequence modeling for optical response retrieval in metasurfaces for STPV applications, *Opt. Mater. Express* 11 (2021) 3178. <https://doi.org/10.1364/OME.424826>.

[80] R. Yan, T. Wang, X. Jiang, X. Huang, L. Wang, X. Yue, H. Wang, Y. Wang, Efficient inverse design and spectrum prediction for nanophotonic devices based on deep recurrent neural networks, *Nanotechnology* 32 (2021) 335201. <https://doi.org/10.1088/1361-6528/abff8d>.

[81] R. Lin, Y. Zhai, C. Xiong, X. Li, Inverse design of plasmonic metasurfaces by convolutional neural network, *Opt. Lett.* 45 (2020) 1362. <https://doi.org/10.1364/OL.387404>.

[82] S. Salman, X. Liu, Overfitting mechanism and avoidance in deep neural networks, *ArXiv Prepr. ArXiv190106566* (2019).

[83] W. Ma, F. Cheng, Y. Liu, Deep-Learning-Enabled On-Demand Design of Chiral Metamaterials, *ACS Nano* 12 (2018) 6326–6334. <https://doi.org/10.1021/acsnano.8b03569>.

[84] K. He, X. Zhang, S. Ren, J. Sun, Identity Mappings in Deep Residual Networks, *CoRR* abs/1603.05027 (2016). <http://arxiv.org/abs/1603.05027>.

[85] C. Fowler, S. An, B. Zheng, H. Li, H. Tang, M. Haerinia, Y. Dong, Y. Zhang, M.Y. Shalaginov, A.M. Agarwal, C. Rivero-Baleine, M. Kang, K.A. Richardson, T. Gu, J. Hu, H. Zhang, A Deep Neural Network Near-Universal Dielectric Meta-Atom Generator, in: OSA Opt. Des. Fabr. 2021 Flat Opt. Free. IODC OFT, Optica Publishing Group, Washington, DC, 2021: p. JW4D.4. <https://doi.org/10.1364/FLATOPTICS.2021.JW4D.4>.

[86] Z. Liu, L. Raju, D. Zhu, W. Cai, A Hybrid Strategy for the Discovery and Design of Photonic Nanostructures, (n.d.).

[87] Y. Dong, S. An, B. Zheng, H. Tang, Y. Huang, M. Haerinia, H. Zhang, Data Collection and Network Design for Deep Learning Based Metasurface Design, in: 2023 Int. Appl. Comput. Electromagn. Soc. Symp. ACES, IEEE, Monterey/Seaside, CA, USA, 2023: pp. 1–2. <https://doi.org/10.23919/ACES57841.2023.10114751>.

[88] R. Hegde, Deep neural network (DNN) surrogate models for the accelerated design of optical devices and systems, in: C.F. Hahlweg, J.R. Mulley (Eds.), Nov. Opt. Syst. Methods Appl. XXII, SPIE, San Diego, United States, 2019: p. 8. <https://doi.org/10.1117/12.2528380>.

[89] A. Ueno, H.-I. Lin, F. Yang, S. An, L. Martin-Monier, M.Y. Shalaginov, T. Gu, J. Hu, Deep-learning designed fabrication-friendly metasurfaces, in: Front. Opt. Laser Sci. 2023 FiO LS, Optica Publishing Group, Tacoma, Washington, 2023: p. FTu1E.3. <https://doi.org/10.1364/FIO.2023.FTu1E.3>.

[90] C. Yeung, B. Pham, R. Tsai, K.T. Fountaine, A.P. Raman, DeepAdjoint: An All-in-One Photonic Inverse Design Framework Integrating Data-Driven Machine Learning with Optimization Algorithms, *ACS Photonics* (2022) acsphotonics.2c00968. <https://doi.org/10.1021/acsphotonics.2c00968>.

[91] J. Jiang, J.A. Fan, Global Optimization of Dielectric Metasurfaces Using a Physics-Driven Neural Network, *Nano Lett.* 19 (2019) 5366–5372. <https://doi.org/10.1021/acs.nanolett.9b01857>.

[92] S. Woo, J. Park, J.-Y. Lee, I.S. Kweon, CBAM: Convolutional Block Attention Module, in: *Comput. Vis. – ECCV 2018 15th Eur. Conf. Munich Ger. Sept. 8–14 2018 Proc. Part VII*, Springer-Verlag, Berlin, Heidelberg, 2018: pp. 3–19. https://doi.org/10.1007/978-3-030-01234-2_1.

[93] R. Socher, D. Chen, C.D. Manning, A. Ng, Reasoning With Neural Tensor Networks for Knowledge Base Completion, (n.d.).

[94] K. Weiss, T.M. Khoshgoftaar, D. Wang, A survey of transfer learning, *J. Big Data* 3 (2016) 9. <https://doi.org/10.1186/s40537-016-0043-6>.

[95] R. Zhu, T. Qiu, J. Wang, S. Sui, C. Hao, T. Liu, Y. Li, M. Feng, A. Zhang, C.-W. Qiu, S. Qu, Phase-to-pattern inverse design paradigm for fast realization of functional metasurfaces via transfer learning, *Nat. Commun.* 12 (2021) 2974. <https://doi.org/10.1038/s41467-021-23087-y>.

[96] H. Salehinejad, S. Sankar, J. Barfett, E. Colak, S. Valaee, Recent Advances in Recurrent Neural Networks, (2018). <http://arxiv.org/abs/1801.01078> (accessed January 24, 2024).

[97] S. Kiranyaz, O. Avci, O. Abdeljaber, T. Ince, M. Gabbouj, D.J. Inman, 1D convolutional neural networks and applications: A survey, *Mech. Syst. Signal Process.* 151 (2021) 107398. <https://doi.org/10.1016/j.ymssp.2020.107398>.

[98] A. Graves, Long Short-Term Memory, in: A. Graves (Ed.), *Supervised Seq. Label. Recurr. Neural Netw.*, Springer Berlin Heidelberg, Berlin, Heidelberg, 2012: pp. 37–45. https://doi.org/10.1007/978-3-642-24797-2_4.

[99] G. Van Houdt, C. Mosquera, G. Nápoles, A review on the long short-term memory model, *Artif. Intell. Rev.* 53 (2020) 5929–5955. <https://doi.org/10.1007/s10462-020-09838-1>.

[100] R. Dey, F.M. Salem, Gate-variants of Gated Recurrent Unit (GRU) neural networks, in: 2017 IEEE 60th Int. Midwest Symp. Circuits Syst. MWSCAS, IEEE, Boston, MA, 2017: pp. 1597–1600. <https://doi.org/10.1109/MWSCAS.2017.8053243>.

[101] Y. Deng, S. Ren, K. Fan, J.M. Malof, W.J. Padilla, Neural-adjoint method for the inverse design of all-dielectric metasurfaces, *Opt. Express* 29 (2021) 7526. <https://doi.org/10.1364/OE.419138>.

[102] C. Doersch, Tutorial on variational autoencoders, *ArXiv Prepr. ArXiv160605908* (2016).

[103] Q. Meng, D. Catchpoole, D. Skillicom, P.J. Kennedy, Relational autoencoder for feature extraction, in: 2017 Int. Jt. Conf. Neural Netw. IJCNN, IEEE, Anchorage, AK, USA, 2017: pp. 364–371. <https://doi.org/10.1109/IJCNN.2017.7965877>.

[104] W. Ma, Y. Liu, A data-efficient self-supervised deep learning model for design and characterization of nanophotonic structures, *Sci. China Phys. Mech. Astron.* 63 (2020) 284212. <https://doi.org/10.1007/s11433-020-1575-2>.

[105] Homeostatic neuro-metasurfaces for dynamic wireless channel management, *Sci. Adv.* (2022).

[106] Ç. Işıl, D. Mengü, Y. Zhao, A. Tabassum, J. Li, Y. Luo, M. Jarrahi, A. Ozcan, Super-resolution image display using diffractive decoders, *Sci. Adv.* 8 (2022) eadd3433. <https://doi.org/10.1126/sciadv.add3433>.

[107] Y. Kiarashinejad, S. Abdollahramezani, M. Zandehshahvar, O. Hemmatyar, A. Adibi, Deep Learning Reveals Underlying Physics of Light–Matter Interactions in Nanophotonic Devices, *Adv. Theory Simul.* 2 (2019) 1900088. <https://doi.org/10.1002/adts.201900088>.

[108] M.I. Shalaev, J. Sun, A. Tsukernik, A. Pandey, K. Nikolskiy, N.M. Litchinitser, High-Efficiency All-Dielectric Metasurfaces for Ultracompact Beam Manipulation in Transmission Mode, *Nano Lett.* 15 (2015) 6261–6266. <https://doi.org/10.1021/acs.nanolett.5b02926>.

[109] Y. Zhang, C. Fowler, J. Liang, B. Azhar, M.Y. Shalaginov, S. Deckoff-Jones, S. An, J.B. Chou, C.M. Roberts, V. Liberman, M. Kang, C. Ríos, K.A. Richardson, C. Rivero-Baleine, T. Gu, H. Zhang, J. Hu, Electrically reconfigurable non-volatile metasurface using low-loss optical phase-change material, *Nat. Nanotechnol.* 16 (2021) 661–666. <https://doi.org/10.1038/s41565-021-00881-9>.

[110] M.Y. Shalaginov, S. An, Y. Zhang, F. Yang, P. Su, V. Liberman, J.B. Chou, C.M. Roberts, M. Kang, C. Ríos, Q. Du, C. Fowler, A. Agarwal, K.A. Richardson, C. Rivero-Baleine, H. Zhang, J. Hu, T. Gu, Reconfigurable all-dielectric metalens with diffraction-limited performance, *Nat. Commun.* 12 (2021) 1225. <https://doi.org/10.1038/s41467-021-21440-9>.

[111] M.Y. Shalaginov, S. An, F. Yang, P. Su, D. Lyzwa, A.M. Agarwal, H. Zhang, J. Hu, T. Gu, Single-Element Diffraction-Limited Fisheye Metalens, *Nano Lett.* 20 (2020) 7429–7437. <https://doi.org/10.1021/acs.nanolett.0c02783>.

[112] T. Ma, M. Tobah, H. Wang, L.J. Guo, Department of Physics, The University of Michigan, Ann Arbor, Michigan 48109, USA, Department of Materials Science and Engineering, The University of Michigan, Ann Arbor, Michigan 48109, USA, Department of Electrical Engineering and Computer Science, The University of Michigan, Ann Arbor, Michigan 48109, USA, Benchmarking deep learning-based models on nanophotonic inverse design problems, *Opto-Electron. Sci.* 1 (2022) 210012–210012. <https://doi.org/10.29026/oes.2022.210012>.

[113] A. Makhzani, J. Shlens, N. Jaitly, I. Goodfellow, B. Frey, Adversarial autoencoders, *ArXiv Prepr. ArXiv151105644* (2015).

[114] X. Han, Z. Fan, C. Li, Z. Liu, L.J. Guo, High-Freedom Inverse Design with Deep Neural Network for Metasurface Filter in the Visible, (2019). <http://arxiv.org/abs/1912.03696> (accessed January 3, 2024).

[115] J.A. Hodge, K.V. Mishra, Amir.I. Zaghloul, Joint Multi-Layer GAN-Based Design of Tensorial RF Metasurfaces, in: 2019 IEEE 29th Int. Workshop Mach. Learn. Signal Process. MLSP, IEEE, Pittsburgh, PA, USA, 2019: pp. 1–6. <https://doi.org/10.1109/MLSP.2019.8918860>.

[116] J.A. Hodge, K. Vijay Mishra, Amir.I. Zaghloul, Multi-Discriminator Distributed Generative Model for Multi-Layer RF Metasurface Discovery, in: 2019 IEEE Glob. Conf. Signal Inf. Process. Glob., IEEE, Ottawa, ON, Canada, 2019: pp. 1–5. <https://doi.org/10.1109/GlobalSIP45357.2019.8969135>.

[117] D. Zhu, Z. Liu, L. Raju, A.S. Kim, W. Cai, Multifunctional Meta-Optic Systems: Inversely Designed with Artificial Intelligence, (n.d.).

[118] J. Jiang, J.A. Fan, Simulator-based training of generative models for the inverse design of metasurfaces, *Nanophotonics* 9 (2020) 1059–1069. <https://doi.org/10.1515/nanoph-2019-0330>.

[119] R.P. Jenkins, S.D. Campbell, D.H. Werner, Establishing exhaustive metasurface robustness against fabrication uncertainties through deep learning, *Nanophotonics* 10 (2021) 4497–4509. <https://doi.org/10.1515/nanoph-2021-0428>.

[120] H. Ahmed, X. Zeng, Y. Wang, H. Bello, N. Iqbal, R. Nordin, Multifunctional Metasurface Polarizers Synthesis Using Effective Data Generation with Adaptive Attention and Space-To-Depth Enhanced Network, *Adv. Opt. Mater.* 12 (2024) 2401220. <https://doi.org/10.1002/adom.202401220>.